Aus der Klinik für Gynäkologie mit

Schwerpunkt gynäkologische Onkologie

der Medizinischen Fakultät Charité-Universitätsmedizin Berlin

DISSERTATION

Characterization of cytotoxic effect by disulfiram in ovarian cancer cell lines

Zur Erlangung des akademischen Grades
Doctor medicinae (Dr. med.)
vorgelegt Medizinischen Fakultät
Charité - Universitätsmedizin Berlin
von
Fang Guo

aus Shanghai, China

Datum der Promotion:

07.12.2018

CONTENTS

ABBREVIATIONS AND ACRONYMS

ADC	Alcohol dehydrogenase
ALDH	Aldehyde dehydrogenase isoform
bFGF	Basic fibroblast growth factor
CFU	Colony-forming units
CSCs	Cancer stem cells
DEAB	Diethylaminobenzaldehyde
DNA	Deoxyribonucleic acid
DMEM	Dulbecco's modified eagle medium
DSF	Disulfiram
EOC	Epithelial ovarian cancer
EGF	Epidermal growth factor
ER	Endoplasmic reticulum
FACS	Fluorescence-activated cell sorter
FBS	Fetal bovine serum
FIGO	International Federation of Gynecology and Obstetrics
FITC	Fluorescein-isothiocyanate
FOXO	Forkhead box O
GSH	Glutathione
HIF1	Hypoxia-inducible transcription factor 1
H_2O_2	Hydrogen peroxide
O_2•–	Superoxide free radicals
HO•	Hydroxyl free radicals
MDC	Monolayer-derived cells

MTT	3-(4,5-dimethylthiazol-2-yl)-2,5-diphenyltetrazolium bromide
NADP+	Nicotinamide-adenine dinucleotide phosphate positive
NADPH	Nicotinamide adenine dinucleotide phosphate hydrogen
PBS	Phosphate-buffered saline
PE	P-phycoerythrin
PerCP	Peridinin chlorophyll protein
PI	Propidium iodide
RA	Retinoic acid
ROS	Reactive oxygen species
SC	Stem cells
SDC	Spheroid-derived cells
SDS	Sodium dodecyl sulfate

Summary

Background: Cancer stem cells (CSCs) are quiescent and slow-cycling cell populations with increased tumorigenicity, unlimited self-renewal ability, and multipotent capacity. They present an explanation for the recurrence and metastasis of cancer. Aldehyde dehydrogenase (ALDH) is a widely accepted CSC marker. Disulfiram (DSF), which is an inhibitor of ALDH, is inexpensive, accessible worldwide, and an approved drug. It is a potentially novel chemotherapeutic agent targeting CSCs.

Methods: The cytotoxic effect of DSF on ovarian cancer cells was demonstrated by MTT assay. Spheroid formation, colony formation, and ALDH activity assay were performed to investigate the inhibitory effect on ovarian cancer stem cells. Cell cycle, cellular apoptosis, and intracellular reactive oxygen species (ROS) were detected by flow cytometry to further explore the mechanism of DSF. The potential of DSF in combination with other chemotherapeutic agents for ovarian cancer treatment was quantitatively assessed.

Results: DSF displayed dose-dependent and time-dependent cytotoxic effects on ovarian cancer cells, and Cu^{2+} significantly enhanced the cytotoxicity. DSF with or without Cu^{2+} significantly inhibited spheroid formation. The average number of spheroids per 200 seeded cells was reduced from 71 to 0 in IGROV1; 16 to 0 in SKOV3; 38 to 0 in SKOV3IP1 ($P<0.01$) in controls and treated cells, respectively. Colony formation capacity was reduced from around 700 cfu in controls to 200 cfu in SKOV3 cell line and from around 1000 cfu to 500 cfu in IGROV1 and SKOV3IP1 cell lines ($P<0.05$). ALDH activity expressed as the proportion of ALDH+ cells was reduced from 21.7% to 0.391% in IGROV1; 8.4% to 0 in SKOV3; 6.88% to 0.05% in SKOV3IP1 ($P<0.05$). DSF induced more intracellular ROS generation in a dose-dependent manner and typically triggered cellular apoptosis. DSF sensitized cisplatin treatment on ovarian cancer cells even at its low concentration (0.3 μM) and significantly enhanced cisplatin-induced cellular apoptosis. DSF showed synergistic effects combined with cisplatin as well as DSF/cisplatin/paclitaxel drug combinations. The concentration of each chemotherapeutic agent in the combinations could be reduced up to hundreds-fold due to this synergistic effect.

Conclusion: Our findings provided strong evidence that DSF modulates ALDH activity and intracellular ROS generation and is enhanced by the addition of Cu^{2+}. It could be a noval candidate adjuvant chemotherapeutic agent in ovarian cancer treatment. Our results indicate synergistic effects of DSF when used in combination with other chemotherapeutic agents, offering hope for patients undergoing traditional chemotherapy who are in dire need of novel treatments that could reduce adverse side effects due to high doses.

Zusammenfassung

Hintergrund: Tumorstammzellen (engl. Cancer stem cells, CSC) sind proliferativ quieszente and langsam proliferierende Zellpopulationen mit erhöhter Tumorigenität, unbegrenzter Selbsterneuerungskapazität und multipotenter Plastizität. Sie stellen eine Erklärung für die Wiedererkrankung an und Metastasierung von Krebs dar. Aldehyddehydrogenase (ALDH) ist ein allgemein akzeptierter CSC Marker. Disulfiram (DSF) ist ein Inhibitor von ALDH, ist billig, weltweit verfügbar und ein zugelassenes Medikament. Potentiell ist es ein neues chemotherapeutisches Agens für CSC.

Methoden: Der zytotoxische Effekt von DSF auf Ovarialkarzinomzellen wurde durch MTT Test gezeigt. Spheroidbildung, Koloniebildung und ALDH Aktivitätstests wurden durchgeführt, um den inhibitorischen Effekt auf Ovarialkarzinomstammzellen zu untersuchen. Zellzyklus, Apoptose und intrazelluläre reaktive Sauerstoffspezies (ROS) wurden mittels Durchflußzytometrie gemessen, um die Wirkmechanismen von DSF weiter zu untersuchen. Mögliche Wirkungen von DSF in Kombination mit anderen Chemotherapiewirkstoffen für Ovarialkarzinombehandlung wurden quantitativ bestimmt.

Ergebnisse: DSF zeigte dosisabhängige und zeitabhängige zytotoxische Effekte auf Ovarialkarzinomzellen, und Cu2+ verstärkte die Zytotoxizität signifikant. DSF mit oder ohne Cu2+ inhibierte die Spheroid-Bildung signifikant. Die durchschnittliche Anzahl von Spheroiden pro 200 ausgesäter Zellen wurde in IGROV1 Zellen von 71 auf 0 reduziert; 16 auf 0 in SKOV3 Zellen; 38 auf 0 in SKOV3IP1 Zellen ($P<0.01$), jeweils in Kontroll- und in behandelten Zellen. Koloniebildungsfähigkeit wurde von ca. 700 cfu in Kontrollzellen auf 200 cfu in SKOV3 Zellen und von ca. 1000 cfu auf 500 cfu in IGROV1 und in SKOV3IP1 Zellen reduziert ($P<0.05$). ALDH Aktivität, ausgedrückt als der Anteil von ALDH+ Zellen, wurde von 21.7% auf 0.391% in IGROV1; 8.4% auf 0 in SKOV3; 6.88% auf 0.05% in SKOV3IP1 ($P<0.05$) reduziert. DSF induzierte mehr intrazelluläres ROS in einer dosisabhängigen Weise und löste typischerweise Apoptose aus. DSF sensibilisierte Ovarialkarzinomzellen für Cisplatin-Behandlung sogar bei niedrigen Konzentrationen (0,3 μM) und erhöhte Cisplatin-induzierte Apoptose signifikant. DSF zeigte synergistische Effekte in Kombination mit Cisplatin wie auch mit DSF/Cisplatin/Paclitaxel Kombinationen. Die Konzentration eines jeden Chemotherapeutikums konnte in den Kombinationen bis zu 100-fach reduziert werden, Dank des synergistischen Effekts.

Schlußfolgerung: Unsere Ergebnisse liefern starke Hinweise darauf, dass DSF die ALDH Aktivität und intrazelluläre ROS Generierung moduliert, was durch die Zufügung von Cu2+ verstärkt wird. Es könnte ein Kandidat für ein neues adjuvantes Chemotherapeutikum für Ovarialkarzinombehandlung sein. Unsere Ergebnisse zeigen synergistische Effekte von DSF in Kombination mit anderen Chemotherapeutika auf, was Hoffnung für traditionelle Chemotherapiepatienten gibt, die einen dringenden Bedarf an neuen Behandlungsoptionen haben, welche unerwünschte Nebenwirkungen durch hohe Dosierung reduzieren könnte.

1. Introduction

1.1 Epithelial ovarian cancer treatment

Epithelial ovarian cancer (EOC) is a highly fatal gynecologic malignancy with the 5-year survival for all stages estimated at 45.6% [1]. This high mortality and morbidity associated with ovarian cancer is mostly due to late diagnosis and resistance to treatment [2]. Around 70% of EOC cases are diagnosed at an advanced FIGO stage(International Federation of Gynecology and Obstetrics) that has already spread within the abdomen, resulting in poor 5-year survival rates [6]. Although many patients initially benefit from surgery and chemotherapy [3,4], recurrence develops in more than 80% of patients with advanced stage and in 25% with early stage disease [5].

Currently, the standard therapy in primary ovarian cancer is surgery followed by systemic administration of a platinum-based chemotherapy (cisplatin or carboplatin) combined with a taxane (paclitaxel or docetaxel) [6,7]. Firstly, cytoreductive surgery remains an accepted standard treatment for primary ovarian cancer. The complete cytoreduction rates range from 9% to 100% in patients with recurrent ovarian cancer [8,9]. However, the benefit of surgery on progression-free survival and overall survival in recurrent ovarian cancer is still controversial. Secondly, platinum-based chemotherapy is commonly used for ovarian cancer, and the major breakthrough in the last decade is the addition of paclitaxel [10]. A combination with platinum and paclitaxel showed higher therapeutic efficacy compared to platinum alone [10].

Although great progress has been made in the chemotherapy of ovarian cancer, obstacles are still there preventing the further development. One problem is the development of resistance to cisplatin. It has been observed that around 50% of the patients relapse within 5 years although they may have achieved good initial response to cisplatin treatment [11]. Another problem is the high cytotoxicity of chemotherapy in patients which limits the wide use in clinic. Cisplatin is a platinum compound that was found to induce DNA damage and arrest cell division [12]. However, due to higher incidence of nephrotoxicity, peripheral nerve toxicity, and inner ear toxicity in patients, its use is still limited [13]. Paclitaxel is a microtubule poison which arrests cells in mitosis [14,15,16], and its dose-limiting toxicity are hypersensitivity, neutropenia, and peripheral neuropathy [17]. Above all, it remains a priority of research to increase the sensitivity to chemotherapy or to better target cancer cells for antitumor drug activity.

1.2 Characteristics of CSCs

Although most ovarian cancer cells initially show a good response to chemotherapy, there is a small subpopulation of cells (generally less than 2% of cells) that are more resistant to initial therapy and could give rise to more differentiated progeny that comprise most of the ovarian tumor mass, leading to a clinical recurrence [18,19,20]. This subpopulation of cells, like normal stem cells, which are responsible for tumorigencity, metastasis, invasion, and chemotherapy resistance, are referred to as cancer stem cells (CSCs).

It is widely accepted that CSCs are a quiescent and slow-cycling cell population possessing self-renewal capacity and giving rise to non-tumorigenic progeny that make up the bulk of the tumor [21,22]. Lapidot and colleagues first isolated a tumorigenic stem cell population in 1994, and showed that one single CSC isolated from acute myeloid leukemia was able to completely reinitiate leukemia in mice [18]. It has also been shown in many types of solid cancer that this small subpopulation of cells is clonogenic both in culture and in vivo [23,24,25,26]. Bapat and colleagues were among the first researchers to demonstrate stem cell properties in ovarian cancer cells in 2005 [27]. It is now generally accepted that cancer stem cells have three basic characteristics: (1) increased tumorigenicity which is responsible for the generation and regeneration of a tumor; (2) unlimited self-renewal which allows CSCs to persist for long periods of time, instead of differentiation and dying after short periods of time like bulk tumor cells; (3) multipotency, whereby tumors that form after CSC injection are composed of both marker-positive and marker-negative cells (ALDH+/-) [28,29].

The existence of CSCs in ovarian cancer makes sense. Firstly, from the aspect of the clinic; although most tumor cells can be killed by the first period by chemotherapy, almost all patients will suffer a recurrence after the outgrowth of a chemotherapy-resistant subpopulation. However, most of these patients at first recurrence will respond well to the secondary therapy, implying that the recurrent tumor is again composed of bulk tumor cells which are sensitive to chemotherapy and CSCs which are more resistant to chemotherapy [29]. Secondly, from the aspect of pathology; epithelial ovarian cancer encompasses numerous histological phenotypes, including papillary serous, endometrioid, clear cell, and mucinous subtypes, implying a pluripotent differentiation capacity. The high rate of multiple “mixed” histological phenotypes within the same tumor suggests either a common cell of origin with capacity to differentiate into several phenotypes or multiple CSC phenotypes [29,30].

Some experiments have also shown that the stemness of CSCs can be induced by chemotherapy or radiation therapy, suggesting the possibility that cells responsible for recurrence might arise from the mutagenic effect of therapy [31]. However, this can't explain why most recurrent tumors are genetically and histologically similar to the primary tumor. In addition, lots of groups have isolated subpopulations and demonstrated that the resistance was present before chemotherapy was given [29]. Above all, these subpopulations of CSCs are closely associated with recurrence, therefore agents specifically targeting these cells may offer a way to minimize the risk of recurrence or maximize the efficacy of chemotherapy.

1.3 Aldehyde dehydrogenase (ALDH) as possible target for novel treatment approaches

Aldehyde dehydrogenases (ALDHs) are a group of nicotinamide-adenine dinucleotide phosphate (NADP+)-dependent enzymes that are critical for detoxification of endogenous aldehyde substrates [32,33]. Endogenous aldehydes arise from the metabolism of amino acids, alcohols, and lipids. Nineteen different ALDH genes with biological functions, including cellular detoxification, have been characterized. They have been found expressed in multiple different tissues and in various cellular subcompartments including cytosol, nucleus, mitochondria, and endoplasmic reticulum [34].

ALDHs play important roles in retinoid signaling, reactive oxygen species (ROS) and acetaldehyde metabolism. In retinoid metabolism, retinol is first oxidized by retinol dehydrogenases to retinal which is then oxidized to retinoic acid (RA) and catalyzed by ALDH1A1, ALDH1A2, ALDH1A3, and ALDH8A1. RA can bind RA receptor and regulate stemness-related marker expression, cellular differentiation and cell cycle arrest [35]. Therefore, the retinoid signaling pathways together with ALDHs play significant roles in stem cell and cancer cell regulation [36,37]. Ethanol is metabolized to acetaldehyde by alcohol dehydrogenase (ADH) which interferes with the antioxidative defense system and generates ROS. Acetaldehyde is then metabolized to acetate by ALDH1A1 and ALDH2. Additionally, studies have shown that ALDH1 can decrease intracellular oxidative stress as it functions as ROS scavenger [38,39]. Thus, ALDHs activity is required to reduce reactive aldehydes and maintain ROS levels sufficiently low, thereby promoting tumor growth and initiating tumorigenesis in CSCs as well as preventing the triggering of CSC apoptosis [40].

There is growing support for the use of ALDH as a CSC marker. Tumor cells with higher ALDH activity have been demonstrated to have enhanced motility and ability to metastasis in many types of cancers [41-46]. ALDH-positive cells have also been reported to exhibit increased capacity to form spheroids in breast cancer, ovarian cancer, brain tumor, prostate cancer, head and neck squamous cell carcinoma, non-squamous cell lung cancer, esophageal cancer, and cervical cancer [47-51]. In addition, ALDH-positive cells display stem-like behavior such as differentiation and resistance to chemotherapy. All the evidence implies that ALDH could be used as a CSC marker and have an important functional role in tumor cell self-protection, expansion, differentiation, and therapy resistance. Therefore, it is expected that novel, potent and ALDH-specific inhibitors could enter the experimental and clinical assessment in cancer therapy in coming years. This suggests that ALDH-specific targeted therapy might be useful for CSC elimination and for combination with traditional chemotherapy.

1.4 Potential anti-tumor effect of DSF

Disulfiram (DSF), a member of the dithiocarbamate family, has been an FDA-approved drug in clinical alcoholism treatment for over 60 years. Initially, the compound had been used in the process of rubber manufacturing. In 1937, workers who were regularly exposed to DSF exhibited flu-like symptoms when they ingested alcohol [52]. DSF, also known as Antabuse, was approved for used in the clinic as an anti-alcoholic treatment since the year of 1948 [53].

With the more recent discovery of stem cell populations in cancer, new purposes and uses were found for DSF. It has been proven that DSF reacts with redox-sensitive sulfhydryl groups (thiols) and binds copper (Cu^{2+}). Thiols are a class of organic sulphur derivatives (mercaptans), distributed ubiquitously in aerobic life forms, and characterized by the presence of sulfhydryl groups (-SH) at their active center which contribute to antioxidant defense mechanisms [54,55]. Cu^{2+} plays an important role in biological pathways in the human body such as to activate some critical proteins like superoxide dismutase, tyrosinase, and cytochrome oxidase [56]. Therefore, Cu^{2+} concentrations in the human body is tightly regulated. However, the concentration of Cu^{2+} in cancerous tissues, such as breast, prostate, lung, and brain, is higher than normal tissues [57]. Thus, it would be useful and practical to study DSF's cytotoxicity in conjunction with intracellular Cu^{2+} participation.

Recent studies have already demonstrated that DSF has strong anticancer activity in vitro and in cancer xenografts [58-61], highlighting it as a potential novel chemotherapeutic agent. DSF is interesting not only because it is a specifically targeting agent which has potential efficacy against the chemo-resistant CSC population but also because it is inexpensive, accessible worldwide and its safety profile has been verified for decades. However, the mechanism of DSF as an ALDH inhibitor for anti-cancer treatment is still unclear. In addition, DSF may support current chemotherapy that is in dire need of novel treatments that could reduce adverse side effects due to high doses. Therefore, investigations need to establish dosing schedules and chemotherapeutic combinations which will generate the greatest response in tumor cells.

1.5 Regulation system of intracellular ROS

Reactive oxygen species (ROS) are broadly defined as oxygen-containing chemical species with reactive properties. These include the superoxide (O_2•−) and hydroxyl (HO•)-free radicals as well as non-radical molecules such as hydrogen peroxide (H_2O_2) [63]. ROS are constantly generated from the oxygen that is consumed in various metabolic reactions with or without enzymatic catalysis [62].

It is fundamental to maintain the redox homeostasis for ensuring cell survival and functions, and this balanced redox status is exerted by ROS that accumulate as a result of ROS generation and elimination. ROS generation systems include the mitochondrial respiratory chain, where a large amount of superoxide is produced by NADPH oxidase complexes [63], or the endoplasmic reticulum (ER) where proteins are engaged to fold into correct conformation and where misfolded proteins will result in ROS accumulation [64]. Hypoxia is also known to stimulate the accumulation of ROS by which the depletion of molecular oxygen could in turn activate hypoxia-inducible transcription factor 1 (HIF1) which has a strong correlation with tumor progression and metastasis [65,66]. ROS-scavenging systems are mainly glutathione (GSH) which is the most abundant non-enzymatic antioxidant molecule in the cell [67], and nicotinamide adenine dinucleotide phosphate hydrogen (NADPH) which is essential for the regeneration of GSH and thioredoxin which have an important role in the elimination of H_2O_2 [62]. Other ROS scavengers such as tumor suppressor genes and ALDH have been proven equally important in response to oxidative stress [39, 68-70].

In biological systems, cellular metabolism is balanced to maintain a stable redox state by ROS generation systems and ROS elimination systems. Once this balance is destroyed, different biological responses will be induced. For example, when ROS is increased at relatively low levels, it could act as a signaling molecule to promote the activation of stress-responsive survival pathways and could be involved in cellular proliferation and differentiation [71,72]. However, a sustained increase in ROS accumulation, regardless of whether it is endogenously or exogenously derived, can be detrimental to cells. Excess amount of ROS causes oxidative damage of lipids, nucleic acids, and amino acids which will lead to cellular dysfunction and death [73]. Therefore, regulating ROS level by ROS generation and elimination systems is critical for cellular function and survival.

1.6 ROS in cancer cells and CSCs

Due to rapid growth and limited availability of nutrients, cancer cells have a high demand for ATP and thus have large consumption of oxygen, and high levels of oxidative stress, resulting in the accumulation of ROS. Numerous studies have proven that compared with their normal counterparts, many types of cancer cells have increased levels of ROS [74,75]. For example, leukaemia cells freshly isolated from blood samples from chronic lymphocytic leukaemia patients showed increased ROS production compared with normal lymphocytes [76].

A diversity of mechanisms is involved in this ROS increase in cancer cells. The intrinsic factors may result from the activation of oncogenes, loss of functional p53, aberrant metabolism, and mitochondrial dysfunction [77-80]. Other factors such as inflammatory cytokines, an imbalance of nutrients and abnormal microenvironment are extrinsic factors known to cause increased ROS accumulation in cancer cells [77,81,82].

Compared with cancer cells, CSCs which are quiescent and slow-cycling cell populations are hypothesized to have low levels of intracellular ROS to maintain their functions such as resistance to radiotherapy and chemotherapy. It has been shown that central nervous system stem cells and hematopoietic stem cells contain lower levels of ROS than their more mature progeny [83,84,85]. Recently, many experiments have proven that CSCs, similar to tissue stem cells, contain lower ROS levels than cancer cells. For example, CD44+CD24-/lowLin- breast CSC-enriched populations contain significantly lower levels of ROS than their non-tumorigenic progeny [86]. Lower levels of ROS are also observed in CSCs in head and neck tumors. As

cancer cells with increased levels of ROS are likely to be more vulnerable to further ROS increase, lower levels of ROS in CSCs and their regulating and detoxification mechanisms would protect them from endogenous and exogenous ROS-mediated damage.

Lower ROS levels in CSCs are associated with increased expression of scavenging systems. For example, glutathione (GSH) which is a critical cellular ROS-reducing agent has been proven to be overexpressed in CSCs [86]. When GSH is depleted by pharmacologic methods, these CSCs become more sensitive to ROS elevation [86]. ALDH has also been shown to be a ROS scavenger that could protect cancer stem cells against oxidative stress induced by alcohol, UV radiation, and some chemotherapeutic agents [87]. In another experiment, the higher mitochondria mass in CSCs may also help to explain the enhanced ROS-scavenging systems as the exposed protein thiols in mitochondrial membranes and in complex I can protect against oxidative damage [88,89].

1.7 Conclusion

Cancer cells with increased oxidative stress are more vulnerable to be damaged by further ROS accumulation. Various drugs that directly or indirectly regulate ROS levels have been used as effective anticancer therapy to selectively kill cancer cells. Here, we focus on DSF which is an inhibitor of ALDH, a functional marker for CSCs, and discuss the inhibitory effect of DSF on ovarian cancer stem cells and its potential modulation of ROS.

Further, as the major problem with chemotherapy is the high toxicity due to high dosage, it is promising to investigate a regimen that could sensitize ovarian cancer cells to cisplatin or maximize cytotoxic effects of chemotherapy while minimizing the side effects on normal tissues. Thus, it is important to investigate the potential of DSF in cancer treatment in combination with other adjuvant therapeutic drugs.

2 Aim of the study

The objective of this thesis was to investigate the cytotoxic effect of DSF on ovarian cancer cells and the possible mechanisms in order to identify the potential of DSF in combination with other chemotherapeutic agents for ovarian cancer treatment. Therefore, the following aims were pursued:

1. To investigate the cytotoxicity of DSF on ovarian cancer cell lines.

2. To investigate the inhibitory effect of DSF on ovarian cancer stem cells in particular, and to further explore its potential cytotoxicity mechanisms.

3. To assess the potential synergism of DSF in combination with other chemotherapeutic agents in ovarian cancer cell lines.

4. To model a new regimen for the treatment of ovarian cancer cells by carrying out computerized quantitative assessment in vitro with combinations of these drugs.

3 Materials

3.1 Laboratory Equipment

Axiovert 40 CFL	Carl Zeiss, Jena, Germany
BD FACSCalibur System	BD Bioscience, Heidelberg, Germany
Freezer, -80°C	Heraeus, Hanau, Germany
Incubator, HERA cell 150	Heraeus, Hanau, Germany
Multicentrifuge	Heraeus, Hanau, Germany
Nanodrop	Peqlab, Erlangen, Germany
Pipettes	Eppendorf AG, Hamburg, Germany
Smart SpecTM Plus Spectrophotometer	BioRad, München, Germany
Thermocycler	Eppendorf AG, Hamburg, Germany
Vortexer	Scientific Industries, N.Y., USA

3.2 Chemicals and Reagents

Agarose	Biozym, Oldendorf, Germany
BD FACSflow^{TM}	BD Sciences, Franklin Lakes, USA
Dimethyl Sulphoxide (DMSO)	Sigma, Deisenhofen, Germany
Ethanol, 70%	Biochrom, Berlin, Germany
Epidermal Growth Factor (EGF)	Biochrom, Berlin, Germany
Fetal bovine serum (FBS)	Gibco BRL, Karlsruhe, Germany
Fibroblast Growth Factor-basic (bFGF)	Biochrom, Berlin, Germany
Penicillin/Streptomycin	Biochrom, Berlin, Germany
Phosphate-buffered saline (PBS) without Mg^{2+}/Ca^{2+}	Biochrom, Berlin, Germany
Trypsin/EDTA Solution	Biochrom, Berlin, Germany

3.3 Cell Culture Media

Dulbecco's modified Eagle's Medium with GlutaMAX™-I (DMEM)	Invitrogen, Heidelberg, Germany
Quantum 263 medium	PAA, Cöllbe, Germany
RPMI 1640	Invitrogen, Heidelberg, Germany

3.4 Kits and other Materials

ALDEFLUOR assay Kit	StemCell Technologies, Köln, Germany
FLUOS-conjugated annexin-V and Propidium iodide Kit	Roche, Mannheim, Germany
Mitosox Red Kit	Invitrogen, Paisley, UK
BD Falcon™ Cell Culture Flasks	BD Bioscience, Franklin Lakes, USA
BD Falcon™ Propylene Conical Tubes	BD Bioscience, Franklin Lakes, USA
BD Falcon™ Tissue Culture Dish (100*200mm)	BD Bioscience, Franklin Lakes, USA
Cell Culture Plates (6-, 24-, 96-well)	BD Bioscience, Franklin Lakes, USA
Ultra-Low Attachment Cell Culture Plate (96-well)	Corning, NY, USA

4 Methods

4.1 Cell lines and cell culture

The ovarian cancer cell lines IGROV1, SKOV3 and SKOV3IP1 were cultured in RPMI 1640 medium with L-glutamine supplemented with 10% fetal bovine serum (heat-inactivated at 56°C for 30 min) and 1% penicillin/streptomycin in a humidified incubator at 37°C and 5% CO_2. All of our experiments were performed on cultures that were 70% confluent.

4.2 Drugs

Free DSF was dissolved in dimethyl sulfoxide (DMSO) at a stock concentration of 10 mM, stored at −20°C and diluted into working concentrations in a corresponding cell culture medium before use.
Cisplatin was kept at a stock concentration of 3.3 mM at room temperature and Paclitaxel was kept at a stock concentration of 7 mM at 4°C. All drugs were diluted into working concentrations with a medium before use.

4.3 Spheroid formation assay

4.3.1 Preparation of ultra-low attachment plates

Agarose was dissolved in PBS at a concentration of 1.5% (w/v). Then, 8 ml of 1.5% agarose was filled into a 75 cm^2 cell culture plate. The plate was gently swirled to make sure that all the agarose covered the plate entirely without any bubbles. Agarose was allowed to solidify and cool down to room temperature for 20 minutes. Thereby, an ultra-low attachment surface on the inner bottom of the plate was prepared.

4.3.2 Preparation of cell suspensions

Adherent monolayer cells were expanded firstly in normal 75 cm^2 culture flasks in RPMI 1640 containing 10% heat-inactivated FBS and 1% penicillin/streptomycin, until 70% confluency. Cells were washed twice with PBS without Ca^{2+}/Mg^{2+} and detached using 3 ml Trypsin/EDTA

for 5-7 minutes until all the cells were detached. The reaction was stopped by addition of 2 ml of complete culture medium. The solution was poured into a 15 ml Falcon tube and centrifuged at 1500 rpm for 5 min. Cells were washed again twice with PBS without Ca^{2+}/Mg^{2+}, followed by resuspension in Quantum 263 medium (PAA) supplemented with 10 ng/ml Epidermal Growth Factor (EGF) and 10 ng/ml Fibroblast Growth Factor-basic (bFGF) and 1% penicillin/streptomycin.

4.3.3 Spheroid formation

The cell number was counted and diluted to 1×10^4 cells/ml in Quantum 263 medium. 10-12 ml of the cell suspensions was transferred into ultra-low attachment cell culture plates. The plates were incubated in a humidified atmosphere with 5% CO_2 at 37°C. Half of the medium was replaced every 3 days. Cell suspensions were left for 10 min to sediment and supernatant was carefully aspirated, leaving the spheroids at the bottom. The same volume of fresh medium was filled into the plates. Movement of the plates was minimized, particularly during spheroid initiation. Cells were allowed to grow for 5-8 days to form spheroids.

4.3.4 Passaging of spheroid

For passaging, all spheroids were collected into a 40 µm mesh filter. They were then washed into a 50 ml Falcon tube, and centrifuged at 1500 rpm for 5 min. Medium was aspirated and spheroids were dissociated into single cells using 500 µl tryspin/EDTA at 37°C 5% CO_2 for 5 min, followed by washing with PBS twice. Single cells were filtered through a 40 µm mesh filter and reseeded in fresh culture medium under same condition. For the experiments generally, 2nd and 3rd generation spheroids were used.

4.3.5 Evaluation of spheroid

Spheroid formation and growth was evaluated and recorded using a HBO50 Microscope. Visualization of spheroid formation, growth, and photographing was done with an AxioCam MRC Zeiss Camera using the AxioVision Rel 4.8 software.

4.4 MTT assay

Adherent cells were harvested using Trypsin/EDTA. A single-cell suspension was prepared as described above and diluted at a concentration of 4×10^4 cells/ml. Cells were reseeded in 96-well plates at a density of 4000 cells per well in 100 µl drug-free medium and incubated overnight. The outer wells of the 96-well plate were filled with 200 µl PBS to create an evaporation barrier.

Serial dilutions of DSF working concentrations were prepared with cell culture medium. The cell culture medium in 96-well plate was removed gently and 100 µl fresh medium was added with various drug concentrations. Each drug concentration was in triplicate. Cells without any drug treatment were used as controls. The 96-well plate was placed in the cell culture incubator for 72 h incubation.

All the cells were checked under the microscope after 72 h incubation. 10 µl of MTT Reagent was added to each well, including controls, and the 96-well plate was incubated at 37°C for 4 hours. When the purple precipitate was clearly visible under the microscope after 4 h incubation, 100 µl stop solution reagent (SDS-HCL) was added to all wells, including controls, and mixed gently. The 96-well plate was left with cover in the incubator overnight. The solution absorbance was measured at wavelength of 590 nm with a Bio-Rad microplate reader.

The average values were determined from triplicate reading wells. Cellular relative viability (%) was calculated according to the equation: Relative viability (%) = (A sample / A control) *100%, where “A sample” and “A control” was the absorbance of the “sample” and “control” wells, respectively. Dose response curves and IC_{50} was calculated using GraphPad Prism 5.04.

4.5 Flow cytometric analysis of the cell cycle

Cells were seeded in 24-well plates at a density of 3×10^4 cells in 1 ml medium per well and incubated overnight. Cells were checked after overnight incubation to make sure the cells were adherent to the bottom of the plates and proliferating. Cells were treated by indicated concentration of DSF and Cu^{2+} for 72 h. Each concentration was in triplicate. Cells without treatment were used as controls.

Cells were harvested after 72 h of incubation as described above, and a single cell suspension was prepared. Cells were washed twice with PBS to remove any residual drug in the medium. Cells were resuspended in 100 µl PBS and fixed by addition of 900 µl 70% ethanol at 4°C overnight. Cells were washed twice with PBS and centrifuged at 3000 rpm for 5 min. Cell loss was carefully avoided when discarding the supernatant especially after ethanol fixation. The cells were then incubated with RNaseA (final concentration 100 µg/ml) and propidium iodide (final concentration 50 µg/ml) for 30 min in the dark at room temperature.

Analysis of cell cycle progression and detection of apoptosis was performed using flow cytometric analysis of DNA staining. The data from 10000 cells for each sample were collected by FACS Scan (BD Bioscience, Heidelberg, Germany) and DNA content and cell cycle was analyzed. First it was gated on the single cell population using pulse width and pulse area, then this gate was applied to forward scatter (FS) and side scatter (SS) to gate out obvious debris. The gates were combined and applied to the PI histogram plot. FlowJo software (Treestar, Ashland, OR, USA) was used to quantitate the percentage of cells in each cell cycle phase (Figure 1).

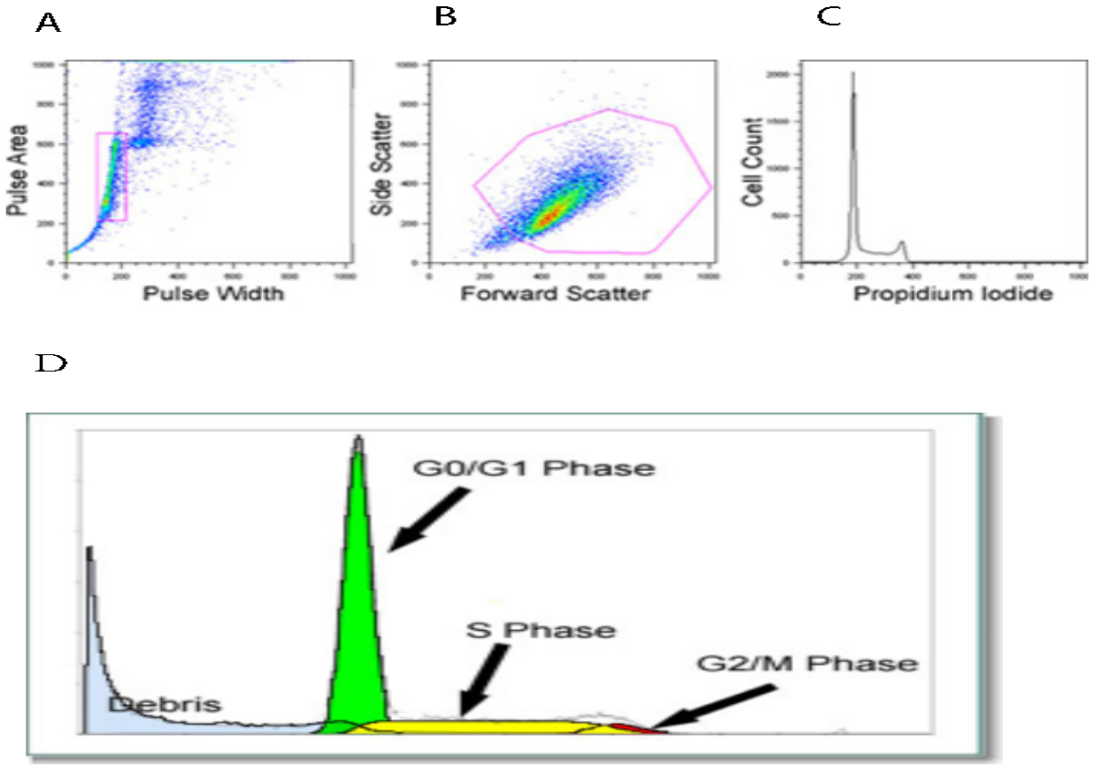

Figure 1: Gating strategy for cell cycle analysis. A) gating a single cell population. B) gating out the debris. C) combining A and B to PI histogram plot. D) cell cycle phases were quantitated by FlowJo software.

4.6 Flow cytometric analysis of cellular apoptosis

4.6.1 Preparation of cells

Cells were seeded in 24-well plates at a density of 4×10^4 cells per well and incubated overnight. Cells were treated with different drugs at different concentration for further 72 h and harvested as described above. Each concentration was in triplicate. Cells without treatment were used as control.

4.6.2 Staining the cells and flow cytometry analysis

The Annexin-V-FLUOS labelling solution was prepared as described in the FLUOS-conjugated annexin-V and propidium iodide Kit (Roche). Cells were washed with PBS twice. The supernatants were discarded, and cells were resuspended in 100 µl of Annexin-V-FLUOS labelling solution at a density of 1×10^6 cells/ml. Cells were incubated in the dark at room temperature for 15 min.

Cellular apoptosis and necrosis were evaluated immediately by flow cytometry with FL3 (propidium iodide) and FL1 (Annexin-V-FLUOS). All cells were divided into four populations: living cells (Annexin V-/ PI-), early apoptotic cells (Annexin V+/ PI-), late apoptotic cells (Annexin V+/ PI+) and necrotic cells (Annexin V-/ PI+).

4.7 Clonogenic assay

Cells were exposed to DSF (1 µM), Cu^{2+} (1 µM), or DSF (1 µM)/Cu^{2+} (1 µM) for 24 h. Cells were harvested after treatment, and washed with PBS twice to make sure all of the residual drug medium was removed. A single cell suspension in fresh medium was prepared and cell numbers were counted. Cells were reseeded in a new 6-well plate at a density of 2000 cells per well with 3 ml fresh cell culture medium in each well. Non-drug-treated cells were included as controls. Each concentration was tested in triplicate.

The 6-well plates were placed in an incubator for 7-10 days until cells in control wells had formed sufficiently large colonies. A cell population was defined as a colony if it consisted of at

least 50 cells. Fixation and staining of colonies was done by adding 2-3 ml of a mixture of 6.0% glutaraldehyde and 0.5% crystal violet. The number of colonies was counted with a microscope.

4.8 Flow cytometric analysis of ALDH activity and cell sorting

4.8.1 ALDEFLUOR kit

ALDH activity is measured by quantifying the ALDH-mediated intracellular retention of fluorescent compound BODIPY-aminoacetate (BAA-) using flow cytometry-based methods [90]. ALDEFLUOR kit was used in the experiment which depends on the conversion of the uncharged ALDH substrate BODIPY amino acetaldehyde (BAAA) into BAA- which is retained inside viable cells. As BAAA could diffuse in and out of the cell freely, after addition of BAAA, cells with elevated activity of ALDH become highly fluorescent and can be identified using flow cytometry gating criteria. Cells treated with diethylaminobenzaldehyde (DEAB) which is a specific ALDH inhibitor, were used as controls.

4.8.2 Treatment of cells

The manufacturer's instructions of ALDEFLUOR kit were closely followed. All tubes were labelled as "test" tubes and one "control" tube. Cells exposed to DSF (10 μM), Cu^{2+} (1 μM), DSF (10 μM) plus Cu^{2+} (1 μM) were all test sample tubes. Cells treated with diethylaminobenzaldehyde (DEAB), which is a specific ALDH inhibitor, were used as control. Then, 1 ml of adjusted test cell suspension ($4*10^4$/ml) was placed into each test sample tube. Then, 5 μl of ALDEFLUOR™ DEAB Reagent was added to the "control" tube, and 5 μl of the activated ALDEFLUOR™ Reagent was added to the "test" tubes. The mixture in the "test" tubes was mixed and 0.5 ml of the mixture was immediately transferred to the DEAB "control" tube. All samples were incubated at 37℃ in the dark for 30 min. After incubation, all tubes were centrifuged at 250*g for 5 min and the supernatant was removed. Cells were resuspended in 0.5 ml of ALDEFLUOR Assay Buffer and stored on ice. Flow cytometric analysis was performed immediately.

4.8.3 Cell sorting

For FACS sorting, cells were suspended in PBS buffer at a concentration of 1×10^7 cells/ml and sorted on an Aria cell sorter (BD Biosciences). The sorted cells were exposed to DSF for 30 min and ROS activity was analyzed by FACS. The sorting gates were established with negative controls which were treated with DEAB.

4.9 Measurement of ROS

Mitochondrial ROS were measured using MitoSOX Red kit (Thermofisher). MitoSOX Red reagent is a novel fluorogenic dye for highly selective detection of superoxide in the mitochondria in live cells. Oxidation of MitoSOX Red reagent by superoxide produces red fluorescence. This fluorescence can be recorded and quantified by flow cytometry.

Following the manufacturer's instructions, cells (4×10^4 cells/well) were seeded in a 24-well attachment plate and incubated overnight. After 24 h plating, tested cells were treated with Cu^{2+} (1 μM), DSF (10 μM), DSF (10 μM) plus Cu^{2+} (1 μM), DSF (100 μM), or DSF (100 μM) plus Cu^{2+} (1 μM) for 30 min at 37 °C. All the medium was removed after drug treatment. Cells were harvested and washed twice with warm PBS. Cells were then incubated with fresh medium containing MitoSOX Red Reagent at a final working concentration of 5 μM for 15 minutes at 37°C. Cells were then washed gently three times with warm buffer.

Mean fluorescence intensity was determined by flow cytometry. Cells without MitoSOX Red Reagent were used as the background. Cells with MitoSOX Red Reagent, but no drug treatment, were used as controls. Mean fluorescence intensity was determined and all samples were normalized to untreated control groups (Figure 2).

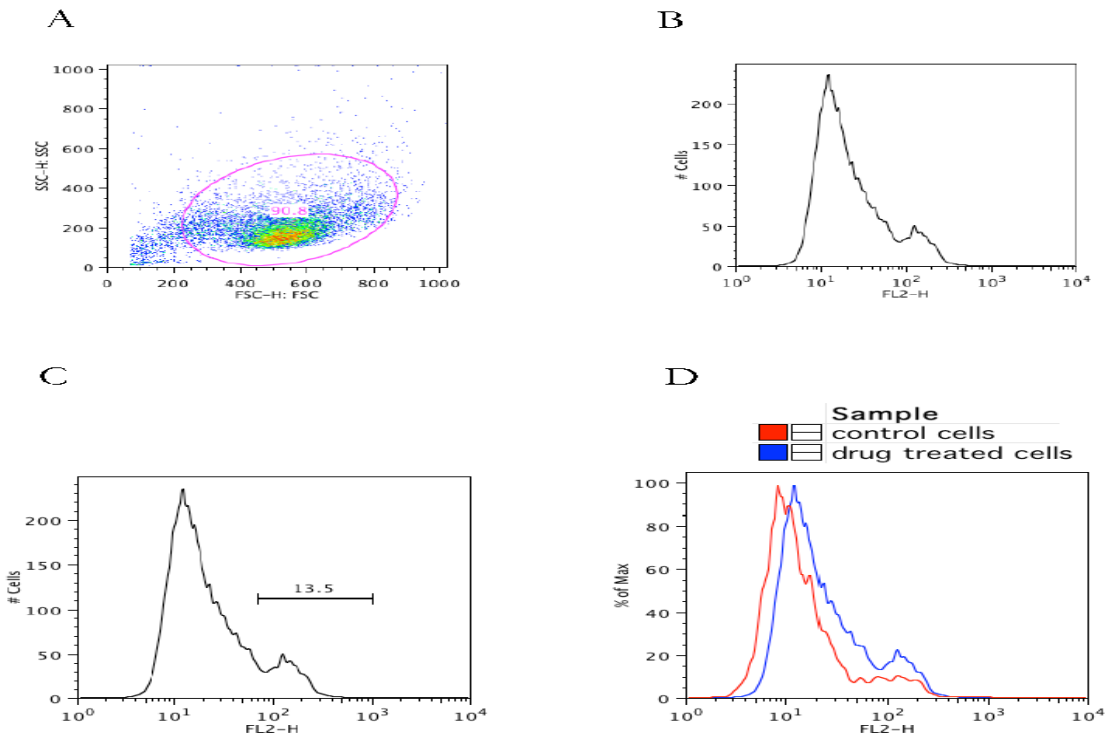

Figure 2: Measurement of ROS by flow cytometry. A) gating out the debris. B) applying to PI histogram plot. C) gating the relative ROS activity. D) drug treated cells were normalized to untreated control cells.

4.10 Drug sensitivity assay

Drug sensitivity assay was done in order to determine whether DSF could sensitize cisplatin treatment. Cells were seeded in 96-well plates at a density of 4000 cells per well in 100 µl drug-free medium and incubated overnight. The outer wells of the 96-well plate were filled with 200 µl PBS to create an evaporation barrier. Cell culture medium was removed and the cells were treated with cisplatin alone at 1 µM or 5 µM, DSF alone at 1 µM or combinations in fresh cell culture medium. Each drug concentration was in triplicate. Cells without any treatment were used as control. The 96-well plate was left with cover in the incubator for 72 h incubation. MTT assay was performed after 72 h incubation.

In another dose-response relationship for this sensitivity assay, cells were treated with cisplatin alone at 0.5 µM, 1 µM, 1.5 µM and 2 µM. Each concentration of cisplatin combined with DSF at 0.3 µM and 0.6 µM. Cells without drug treatment were used as control. Each sample was tested in triplicate. MTT assays were performed after 72 h of drug exposure.

4.11 Double and triple drug combination treatment

The drug combination experiment was designed according to a method published by Chou-Talalay et al. which has been widely accepted and cited in papers [91]. The combination index isobologram method provides the common link between single drug and multiple drug treatments. It is based on the median-effect equation and is used for computerized data analysis which is more accurate and more flexible. This method was selected because it takes into account both the potencies of each drug and the combinations of these drugs.

For each cell line, the dose ranges were selected to cover the concentrations below and above the IC_{50} values of each drug to include the wide concentration ranges for each drug. The combination ratio was designed at a constant ratio which was approximately IC_{50} concentration for each of the component drugs, so that the contribution of the effect by each drug to the combination would be equal [91]. Cells were treated with every single drug or every two drug combinations or all three drugs combination for 72 h and then subjected to MTT assay as described above (Table 1). Each concentration or each combination was tested in triplicate.

For the combination effect analyses, description of synergism or antagonism was based on computer software by Chou and Martin [92]. Briefly, the combination index (CI) value in a combination is a quantitative measure of the degree of drug interaction in terms of synergism or antagonism for a given measurement effect. CI $<$ 1, $=$1, and $>$1 indicate synergism, additive effect, and antagonism, respectively [91]. The smaller the number, the stronger the synergism. Dose-reduction index (DRI) values is a measure of how many fold the dose of each drug in a synergistic combination may be reduced at a given effect level when compared with the doses of each drug alone [91].

Table 1: Double and triple drug combination design

Drug 1				Drug 2				Drug 3		
0.25	*	IC_{50}		0.25	*	IC_{50}		0.25	*	IC_{50}
0.5	*	IC_{50}		0.5	*	IC_{50}		0.5	*	IC_{50}
	IC_{50}				IC_{50}				IC_{50}	
2	*	IC_{50}		2	*	IC_{50}		2	*	IC_{50}
4	*	IC_{50}		4	*	IC_{50}		4	*	IC_{50}
Drug 1 + Drug 2										
0.25	*	IC_{50}	+	0.25	*	IC_{50}				
0.5	*	IC_{50}	+	0.5	*	IC_{50}				
		IC_{50}	+	IC_{50}						
2	*	IC_{50}	+	2	*	IC_{50}				
4	*	IC_{50}	+	4	*	IC_{50}				
Drug 2 + Drug 3										
				0.25	*	IC_{50}	+	0.25	*	IC_{50}
				0.5	*	IC_{50}	+	0.5	*	IC_{50}
						IC_{50}	+	IC_{50}		
				2	*	IC_{50}	+	2	*	IC_{50}
				4	*	IC_{50}	+	4	*	IC_{50}
Drug 1 + Drug 3										
	0.25	*		IC_{50}	+	0.25	*	IC_{50}		
	0.5	*		IC_{50}	+	0.5	*	IC_{50}		
				IC_{50}	+	IC_{50}				
	2	*		IC_{50}	+	2	*	IC_{50}		
	4	*		IC_{50}	+	4	*	IC_{50}		
Drug 1 + Drug 2 + Drug 3										
0.25	*	IC_{50}	+	0.25	*	IC_{50}	+	0.25	*	IC_{50}
0.5	*	IC_{50}	+	0.5	*	IC_{50}	+	0.5	*	IC_{50}
		IC_{50}	+			IC_{50}	+			IC_{50}
2	*	IC_{50}	+	2	*	IC_{50}	+	2	*	IC_{50}
4	*	IC_{50}	+	4	*	IC_{50}	+	4	*	IC_{50}

4.12 Experiments to verify calculated DRI values

To further verify the capability of DSF in potentiating chemotherapy, ovarian cancer cell lines were treated with traditional anti-tumor agents Cisplatin and Paclitaxel or their combination in conjunction with or without DSF. Cisplatin (original IC_{50}), and Paclitaxel (original IC_{50}), DSF (original IC_{50}) were determined firstly from MTT assay for each of the cell lines. According to DRI in the quantitative combination measurement, "reduced IC_{50}" for each drug could be calculated as well, which means that "reduced IC50" of Cisplatin or Paclitaxel could reach the same cytotoxic effect once combined with DSF.

Series of concentrations for single drug and drug combinations were chosen for testing the cells. Cisplatin (original IC_{50}), Cisplatin (reduced IC_{50}), Paclitaxel (original IC_{50}), Paclitaxel (reduced IC_{50}), Cisplatin (original IC_{50}) + Paclitaxel (original IC_{50}), Cisplatin (reduced IC_{50}) + Paclitaxel (reduced IC_{50}), as well as all the single drug or two drug combinations in conjunction with DSF-IC_{50}. All the samples were treated in 96-well plates in an incubator for 72 h, and then MTT assay was performed. Untreated control groups were included in all experiments.

5 Results

5.1 Disulfiram exhibits dose-dependent cytotoxicity in ovarian cancer cell lines

Initially, the cytotoxic effect of DSF on three ovarian cancer cell lines was examined using MTT assay in order to determine the IC_{50} of cytotoxicity for each cell line. As shown in Figure 3, the proliferation of cells was significantly inhibited after exposure to concentrations of DSF between 0.001 μM to 100 μM for 72 h. A dose-dependent cytotoxicity was observed in all three ovarian cancer cell lines. DSF showed linear higher cytotoxicity with increasing concentration of the drug in SKOV3 cell line, and biphasic cytotoxicity in IGROV1 and SKOV3IP1 cell lines, with the relative viability of cells increasing slightly at 10 μM DSF.

IC_{50} values for these three cell lines were calculated:

$IC_{50\text{-IGROV1}}$: 2.01 ± 0.11 μM;

$IC_{50\text{-SKOV3}}$: 0.19 ± 0.09 μM;

$IC_{50\text{-SKOV3IP1}}$: 10 ± 2:48 μM.

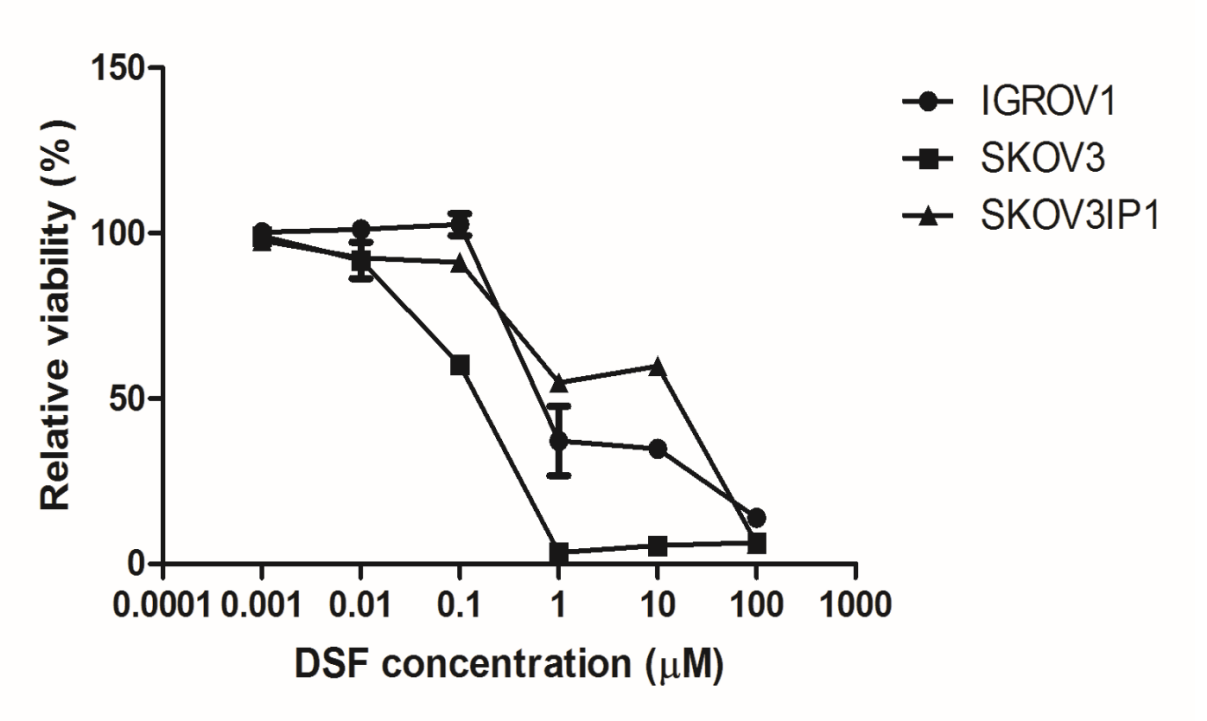

Figure 3: Disulfiram displays dose-dependent cytotoxic effects on ovarian cancer cell lines. The ovarian cancer cell lines were exposed to different concentrations of DSF from 0.001 μM to 100 μM for 72 h followed by MTT assay. One representative of three independent experiments is shown.

5.2 Disulfiram exhibits time-dependent cytotoxicity in ovarian cancer cell lines

We next examined the relationship of time and apoptosis induced by DSF in a time course experiment. The cells were exposed to a certain concentration according to their IC_{50} (IGROV1 and SKOV3IP1: DSF 1 µM; SKOV3: DSF 0.1 µM) for 4-72 h. Flow cytometric analysis with Annexin-V/PI dual staining was performed to determine the percentage of apoptotic cells. As shown in Figure 4, both early apoptosis (Annexin-V+/PI−, lower/right quadrant) and late apoptosis (Annexin-V+/PI+, upper/right quadrant) increased with longer time of treatment. The control cells which were cultured for 72 h without any drug treatment showed less apoptosis than drug-treated cells. Taken together, these results indicate that DSF itself is cytotoxic in a dose-dependent and time-dependent manner around the concentration of their IC_{50} with some variation between the three investigated cell lines.

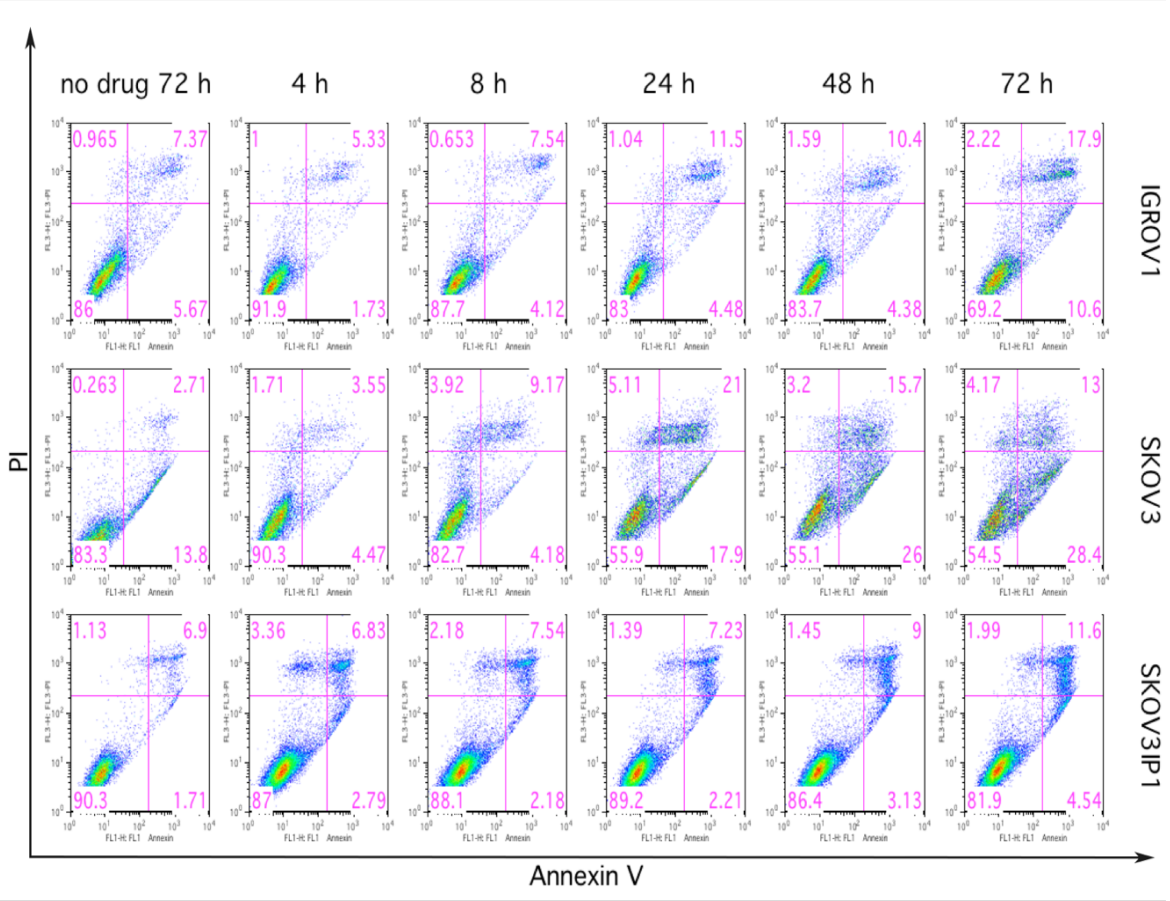

Figure 4: Disulfiram displays time-dependent cytotoxic effects on ovarian cancer cell lines. Ovarian cancer cell lines were exposed to DSF for different duration of treatment time, followed by flow cytometric analysis with Annexin V/PI staining. Cells cultured for 72 h without drug treatment were used as control. One representative of three independent experiments is shown.

5.3 DSF/Cu^{2+} synergistically enhance cytotoxicity on ovarian cancer cell lines

Cells were treated with DSF alone (concentration range from 0.001 μM to 100 μM), Cu^{2+} alone (1 μM), or DSF (concentration range from 0.001 μM to 100 μM) combined with Cu^{2+} (1 μM) in a 96-well plate and incubated for 72 h, followed by MTT assay. Cells without drug treatment were used as control. Each concentration was applied in triplicate.

As shown in Figure 5A, DSF alone showed a significant cytotoxic effect on the three ovarian cancer cell lines as described above. Relative viability of the cells had a sharp decrease at a concentration of 1 μM DSF and all cells died at 100 μM DSF. When 1 μM of Cu^{2+} was added to the DSF, the cytotoxicity of DSF was significantly enhanced. Relative viability started to decrease even at 0.01 μM DSF and a sharp decrease was observed at 0.1 μM DSF when combined with 1 μM Cu^{2+}. At a concentration of 1 μM DSF supplemented with 1 μM Cu^{2+}, almost all the cells died. There was a rebound at 10 μM DSF alone in SKOV3IP1 cell line, and this "protective" effect at 10 μM was totally overcome when DSF was combined with copper, leaving all cells dead at this concentration. No cytotoxicity of Cu^{2+} alone was observed in ovarian cancer cell lines until the cells were treated with 100 μM Cu^{2+}. The results indicated that although DSF alone had significant effects, the cytotoxicity of DSF was significantly enhanced in Cu^{2+} (1 μM)-supplemented medium in all ovarian cancer cell lines.

We then tested the apoptosis of cells treated with DSF alone (1 μM), Cu^{2+} alone (1 μM), and DSF (1 μM)/ Cu^{2+} (1 μM). Cells were treated in 24-well plates and incubated for 72 h. Cells without treatment after 72 h incubation were used as control. Annexin V/PI assay was used to determine apoptosis of cells as described above.

As shown in Figure 5B, both early apoptosis (Annexin V+/PI−, lower right quadrant) and late apoptosis (Annexin V+/PI+, upper right quadrant) as well as necrosis (Annexin V−/PI+, upper left quadrant) increased significantly with DSF/Cu^{2+} treatment compared to DSF alone in three ovarian cancer cell lines.

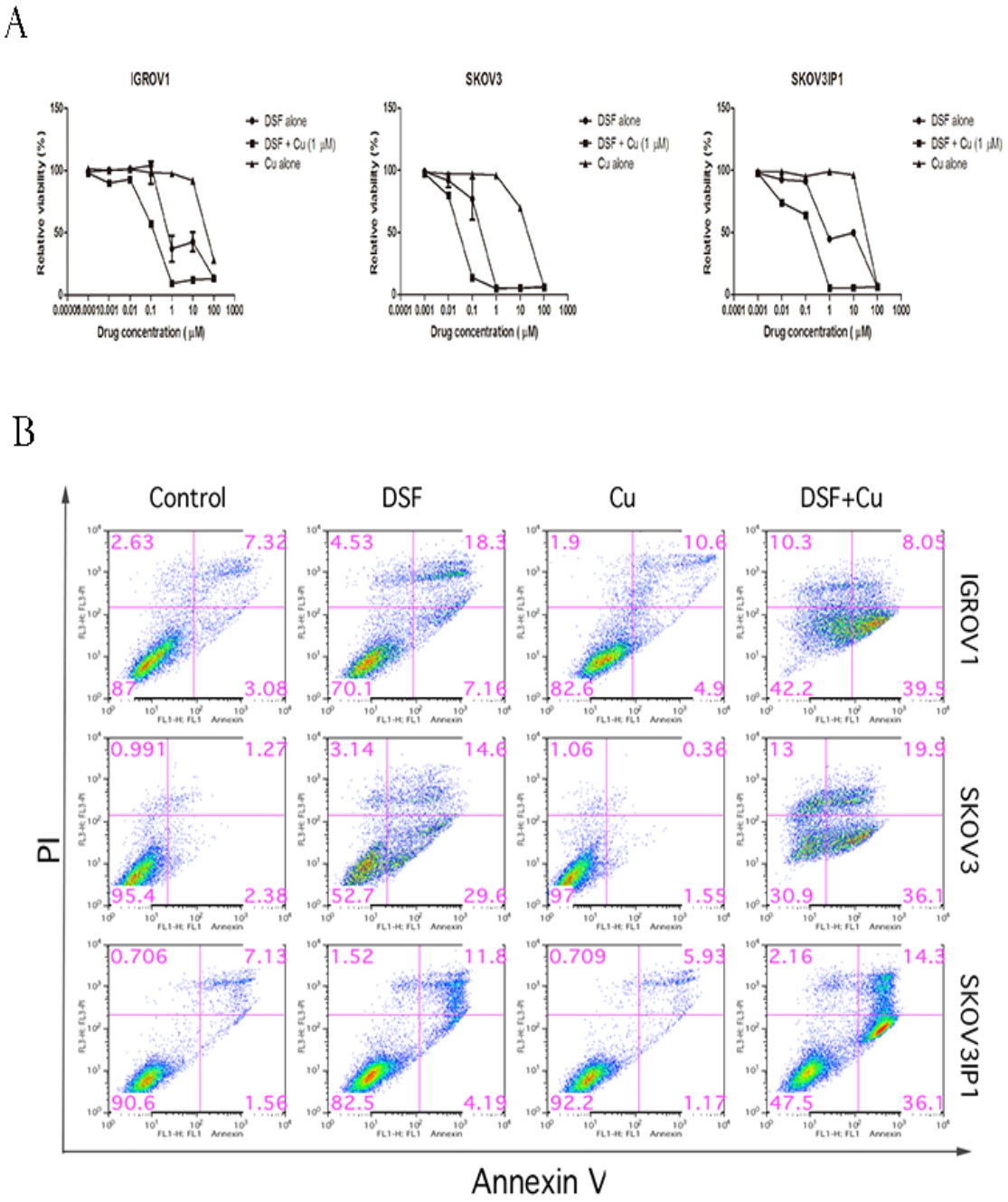

Figure 5: DSF/Cu^{2+} synergistically enhance the cytotoxicity on ovarian cancer cell lines. A). MTT assay. The ovarian cancer cell lines were exposed to different concentrations of DSF combined with 1 μM Cu^{2+} for 72 h. Relative viability (%) was expressed as a percentage relative to the untreated control cells. B). Annexin V/PI assay. Ovarian cancer cells were exposed to 1 μM DSF alone, or 1 μM Cu^{2+} alone, or 1 μM DSF plus 1 μM Cu^{2+} for 72 h. Cells after 72 h culture without treatment were used as control. One representative of three independent experiments.

5.4 No significant cell cycle changes are induced by DSF/Cu^{2+}

As the mechanisms of the cytotoxic effect of DSF with or without Cu^{2+} are still not fully understood, we first tested the damaging effect of DSF on DNA to see if DSF could affect the cell cycle and trigger cell death via apoptosis like other antitumor agents such as cisplatin. Cells were treated with subtoxic doses of DSF alone (0.01 μM) or Cu^{2+} alone (1 μM) or DSF (0.01 μM) plus Cu^{2+} (1 μM) in 24-well plates for 72 h. Cells cultured for 72 h without any treatment were used as control. Analysis of cell cycle was performed using flow cytometric analysis of DNA staining as described in the methods section.

As shown in Figure 6, G1 phase which represents the growth phase starts from the end of the previous M phase until the beginning of DNA synthesis. During this phase, cells grow by increasing their content of proteins and the number of organelles. After DSF/Cu^{2+} treatment, there was a slight decrease in G1 phase in the IGROV1 cell line (from 72.8% to 60.9%) and in the SKOV3 cell line (from 35.2% to 28%). However, there are almost no significant changes in DSF-treated groups in any cell lines. S phase is the DNA replication phase. During this phase, the amount of DNA in the cells is doubled. There was a slight increase in the SKOV3 cell line after DSF treatment (from 30.2% to 38.5%) and DSF/Cu^{2+} treatment (from 30.2% to 34.5%) as well as in the SKOV3IP1 cell line after DSF treatment (from 5.49% to 10.5%) and DSF/Cu^{2+} treatment (from 5.49% to 8.56%). For all other groups treated by DSF+/- Cu^{2+}, there were almost no changes. G2 phase and M phase is a period of protein synthesis and the cellular mitosis phase. No significant change was observed in the G2/M phase. Results above indicated that DSF with or without Cu^{2+} had little effect on cell cycle. DSF did not play an important role in altering the cell cycle.

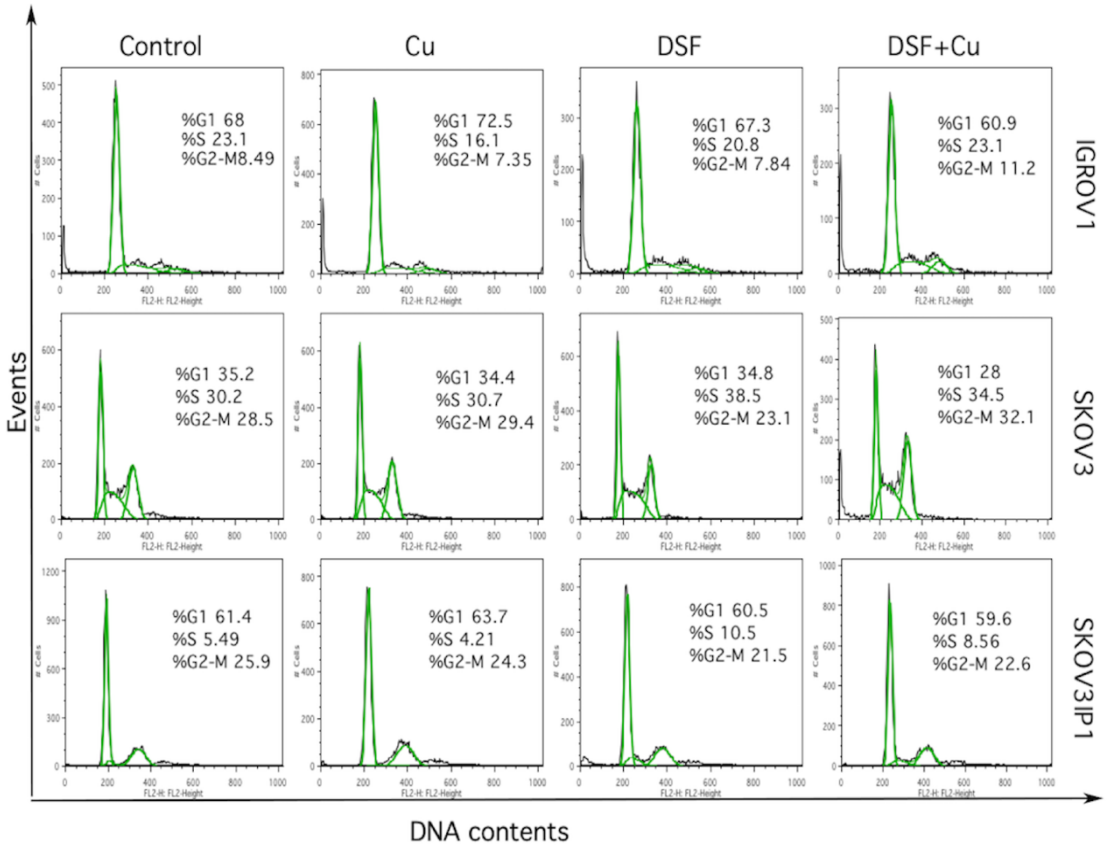

Figure 6: Flow cytometric analysis of cell cycle. Cells were treated with DSF alone or Cu^{2+} alone or DSF plus Cu^{2+} for 72 h. Cells without any drug treatment were used as control. The percentage of cells in each cell cycle phase was quantitated by FlowJo software. One representative of three independent experiments is shown.

5.5 DSF inhibits the formation of spheroids

Spheroid formation assay is a useful method to explore the role of CSCs because the spheroid culture model better imitates in vivo conditions for the spontaneous aggregation of cancer cells. Spheroid-derived cells have been proven to be enriched for CSC or cells with stem cell- related characteristics. Thus, spheroid formation assay has gained wide popularity in CSC research. Here, we used a spheroid formation assay to explore the effect of DSF on CSCs at the single cell level.

Spheroid-derived cells were treated with 0.1 µM DSF or 1 µM Cu^{2+} or 0.1 µM DSF plus 1 µM Cu^{2+} in a 96-well ultra-low attachment plate (200 cells in 0.2 ml medium/well) for 7-10 days. Cells without drug treatment were used as control. Figure 7A shows an abundance of large

spheroids was formed by untreated control cells. The size and shape of the spheroids differed depending on the cell line. The spheroids were quite irregular and smaller in IGROV1 cell line than in the other two cell lines. The ability of ovarian cancer cells to form spheroids was reduced when exposed to DSF. Cells only aggregated, indicating reduced proliferative potential of stem cells. When DSF was combined with 1 μM Cu^{2+}, only diffuse individual cells were observed in DSF/ Cu^{2+}-treated samples and spheroid formation in all three cell lines was completely abolished. Figure 7B shows that the number of spheroids was significantly reduced from average 71 to 0 in IGROV1, from average 16 to 0 in SKOV3, and from 38 to 0 in SKOV3IP1 when the cells were exposed to DSF or DSF/Cu^{2+} ($P<0.01$). Although the numbers of spheroids were slightly reduced in Cu^{2+}-treated cells, there was no significant difference when compared to control cells.

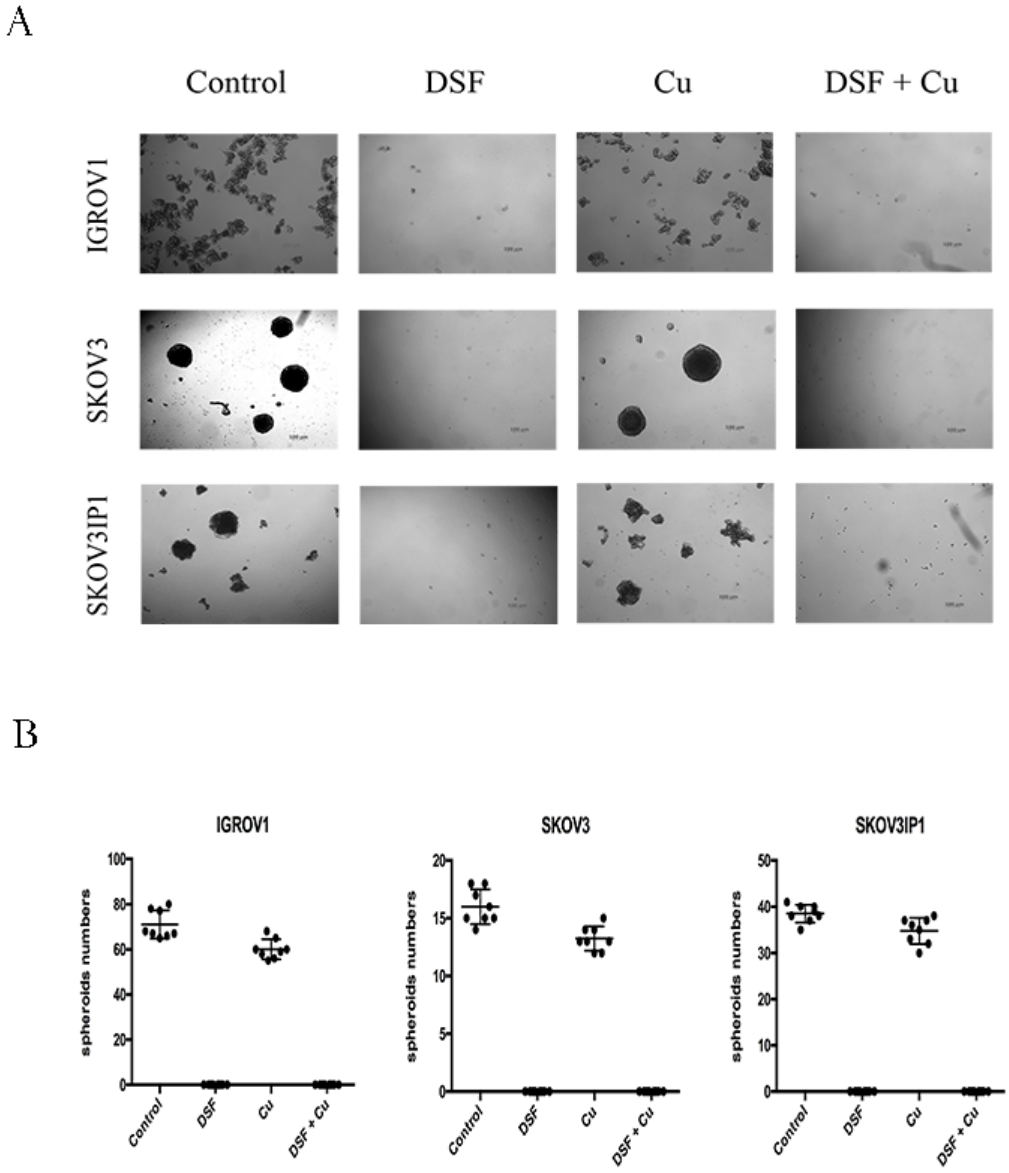

Figure 7: Inhibitory effect of DSF/Cu^{2+} on spheroid formation in ovarian cancer cell lines. A) Cells were treated with 0.1 µM DSF or 1 µM Cu^{2+} or 0.1 µM DSF plus 1 µM Cu^{2+} in ultra-low attachment 96-well plates for 7-10 days and photographed at 50-fold magnification. B) Cells were exposed to drugs for 10 days, and spheroids with ≥100 µm in diameter were counted, and their numbers per well (n=8) were plotted. One representative of three independent experiments is shown.

5.6 DSF/Cu^{2+} inhibits clone formation of ovarian cancer cell lines

The clonogenicity assay was used to detect if the tumor cells retained their reproductive stemness capacity after drug treatment. Here, we tested whether DSF could reduce the clonogenic capacity of the tumor cells. The effect of DSF on CSCs at the single cell level was

determined by the clone formation assay. A colony is defined as a cluster of at least 50 cells arising from a single cell that can be detected by microscopy.

As shown in Figure 8, the colony-forming number in the Cu^{2+} (1 μM) treated group was decreased as compared to control cells which were not treated. This was caused by a slowed growth of surviving cells and resulted in small colonies that did not reach the counting threshold (50 cells per colony). The colony number was significantly more reduced by DSF (1 μM) treatment of cells with colony-forming units from around 700 in control to 200 in the SKOV3 cell line and from around 1000 in control to 500 in the IGROV1 and SKOV3IP1 cell lines ($P<0.05$). The colony-forming ability of ovarian cancer cells was almost totally eradicated by treatment with DSF (1 μM) plus Cu^{2+} (1 μM) in SKOV3 and SKOV3IP1 cell lines. These results indicated that DSF was able to suppress clonogenicity of ovarian cancer cells, and that addition of Cu^{2+} increased the effect.

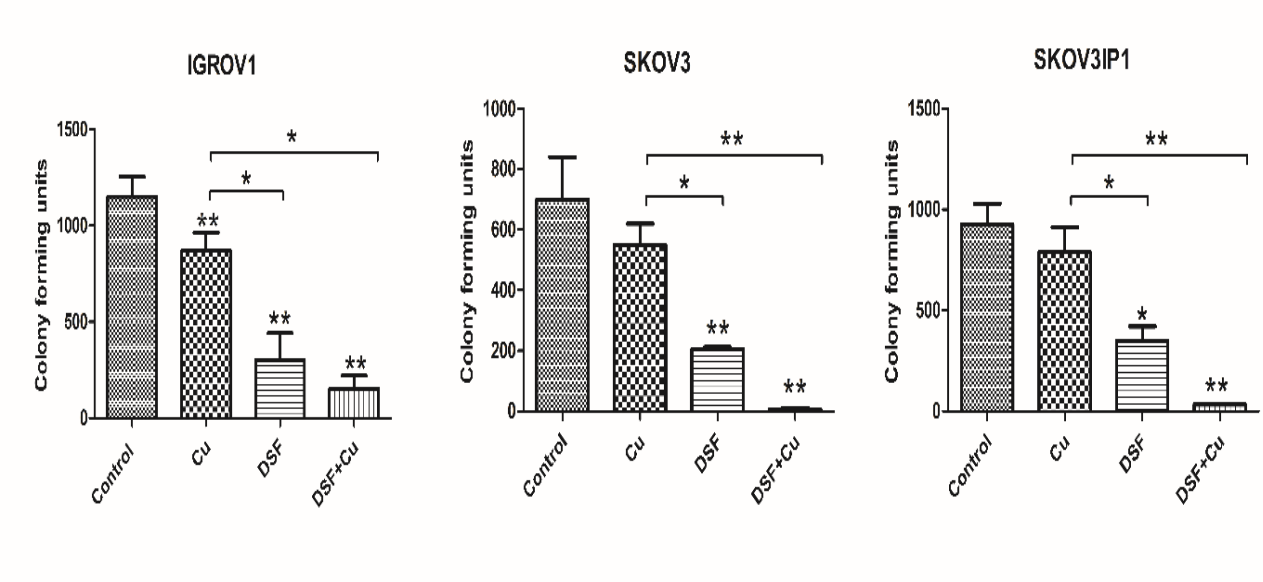

Figure 8: Inhibitory effect of DSF/Cu^{2+} on clonogenicity in ovarian cancer cell lines. The cells exposed to 1 μM Cu^{2+} alone, or 1 μM DSF alone, or 1 μM DSF plus 1 μM Cu^{2+} for 24 h were cultured further in drug-free medium in six-well plates at a cell density of 2000 cells per well for 7-10 days. The colonies were counted microscopically. One representative of three independent experiments is shown. * $P<0.05$. ** $P<0.01$

5.7 DSF/Cu^{2+} inhibits ALDH activity

As ALDHs are important for maintenance and differentiation of stem cells as well as normal development, and increased ALDH activity has been found to relate with stemness of CSCs as

well as chemotherapy resistance, we wanted to determine whether DSF or DSF/Cu^{2+} could inhibit the activity of the aldehyde dehydrogenase enzymes measured by ALDEFLUOR assay.

Figure 9 shows that DSF with or without Cu^{2+} supplementation significantly reduced the proportion of ALDH+ cells detected by ALDEFLUOR assay (from 21.7% to 0.391% in IGROV1; from 8.4% to 0 in SKOV3; from 6.88% to 0.05% in SKOV3IP1), while Cu^{2+} alone did not affect the ALDH+ population. In comparison with control cells which had not been drug treated, the ALDH+ population in cultures with DSF (10 μM)/Cu^{2+} (1 μM) exposure was significantly reduced in ovarian cancer cell lines. It demonstrated that ALDH activity in ovarian cancer cells was inhibited not only by diethylaminobenzaldehyde (DEAB), a specific ALDH inhibitor, but also by DSF with or without Cu^{2+} supplementation. Moreover, the inhibitory effect by DSF was better than that of DEAB, while Cu^{2+} supplementation even enhanced this inhibitory effect compared to DSF alone.

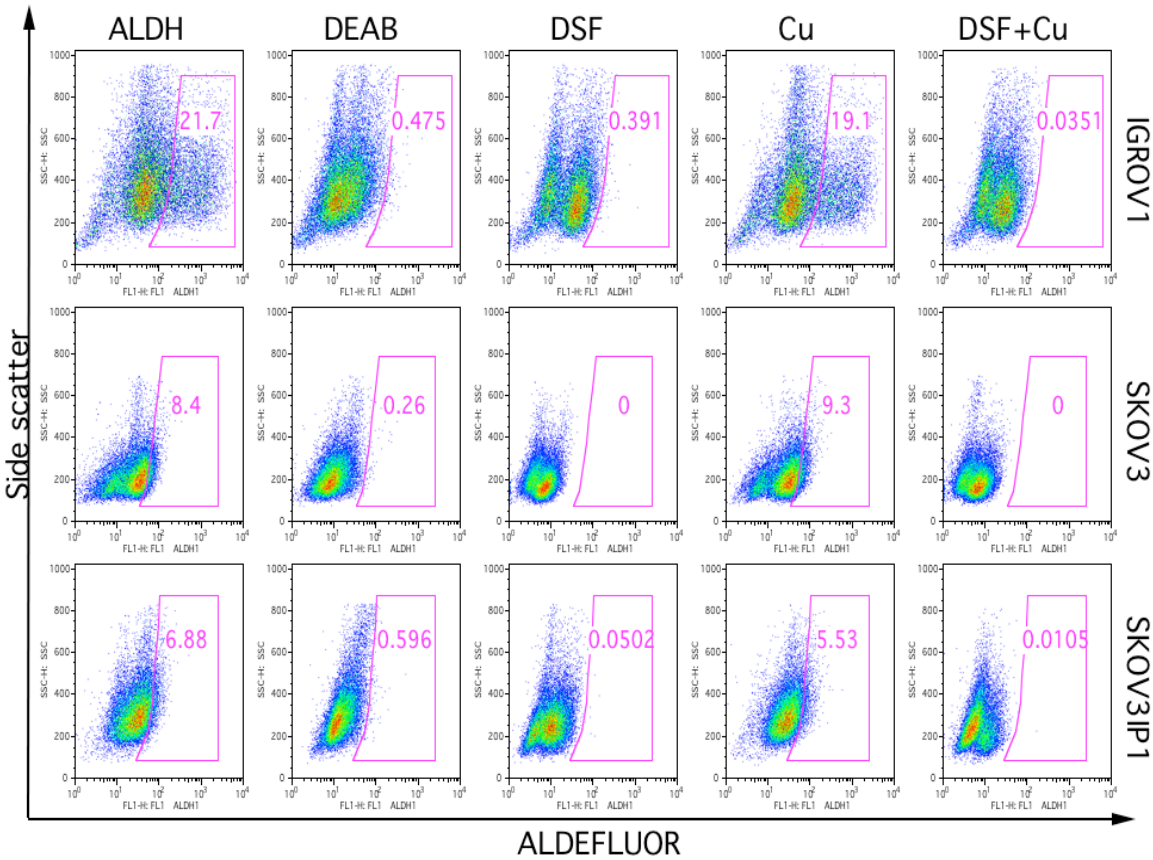

Figure 9: DSF/Cu^{2+} inhibits ALDH activity in ovarian cancer cell lines. Cells were incubated with DSF (10 μM), or Cu^{2+} (1 μM), or DSF (10 μM) plus Cu^{2+} (1 μM), as well as DEAB which was used to establish the baseline fluorescence and define ALDEFLUOR-positive cells (gated cell population). The inserted numbers in the frame represent the percentage of ALDH+ cells. One representative of three independent experiments is shown.

5.8 DSF/Cu^{2+} triggers the generation of ROS, and higher ROS is generated in ALDH+ cells

ROS are involved in cancer development and metastasis via cancer-associated pathways. Agents that increase or decrease the ROS production could affect cancer treatment, leading to a preferential killing of cancer cells. Here, as DSF could inhibit ALDH activity which acts as a ROS scavenger, it is logical to investigate the underlying mechanism of DSF effect based on ROS production.

Three ovarian cancer cell lines were exposed to Cu^{2+} (1 μM), or DSF (10 μM), or DSF (10 μM) / Cu^{2+} (1 μM), or DSF (100 μM), or DSF (100 μM) / Cu^{2+} (1 μM) for 30 min, followed by FACS-based ROS assay analysis and relative mean fluorescence intensity was calculated and normalized to control. As shown in Figure 10A, DSF, with or without Cu^{2+} supplementation, significantly induced ROS activity in all three ovarian cancer cell lines. The relative ROS content after normalization to untreated control cells was increased by 19.4-fold in IGROV1 cell line, 2.98-fold in SKOV3 cell line and 2-fold in SKOV3IP1 cell line in groups treated with DSF 10 μM versus the non-treated control group. More ROS was generated when the DSF concentration was increased from 10 μM to 100 μM. The relative ROS content after normalization to untreated control cells was significantly increased by 64.9-fold in IGROV1, 99.4-fold in SKOV3 and 51.2-fold in SKOV3IP1 in groups treated with 100 μM DSF. With the same concentration of DSF, more ROS was induced by supplementation with Cu^{2+} (1 μM) as compared to DSF treatment alone.

Next, ROS levels in ALDH+ cells and ALDH- cells after DSF treatment were compared to further investigate the effect on CSCs. Cells were treated with 10 μM DSF or 100 μM DSF immediately after cell sorting by ALDEFLUOR, followed by FACS analysis. As shown in Figure 10B, ALDH+ cells exhibited low basal levels of ROS due to higher levels of ALDH expression which is generally a ROS scavenger. However, there was even more ROS generated in ALDH+ cells after 10 μM DSF treatment than in ALDH- counterparts. When DSF concentration was increased to 100 μM, however, ROS levels decreased in ALDH+ cells.

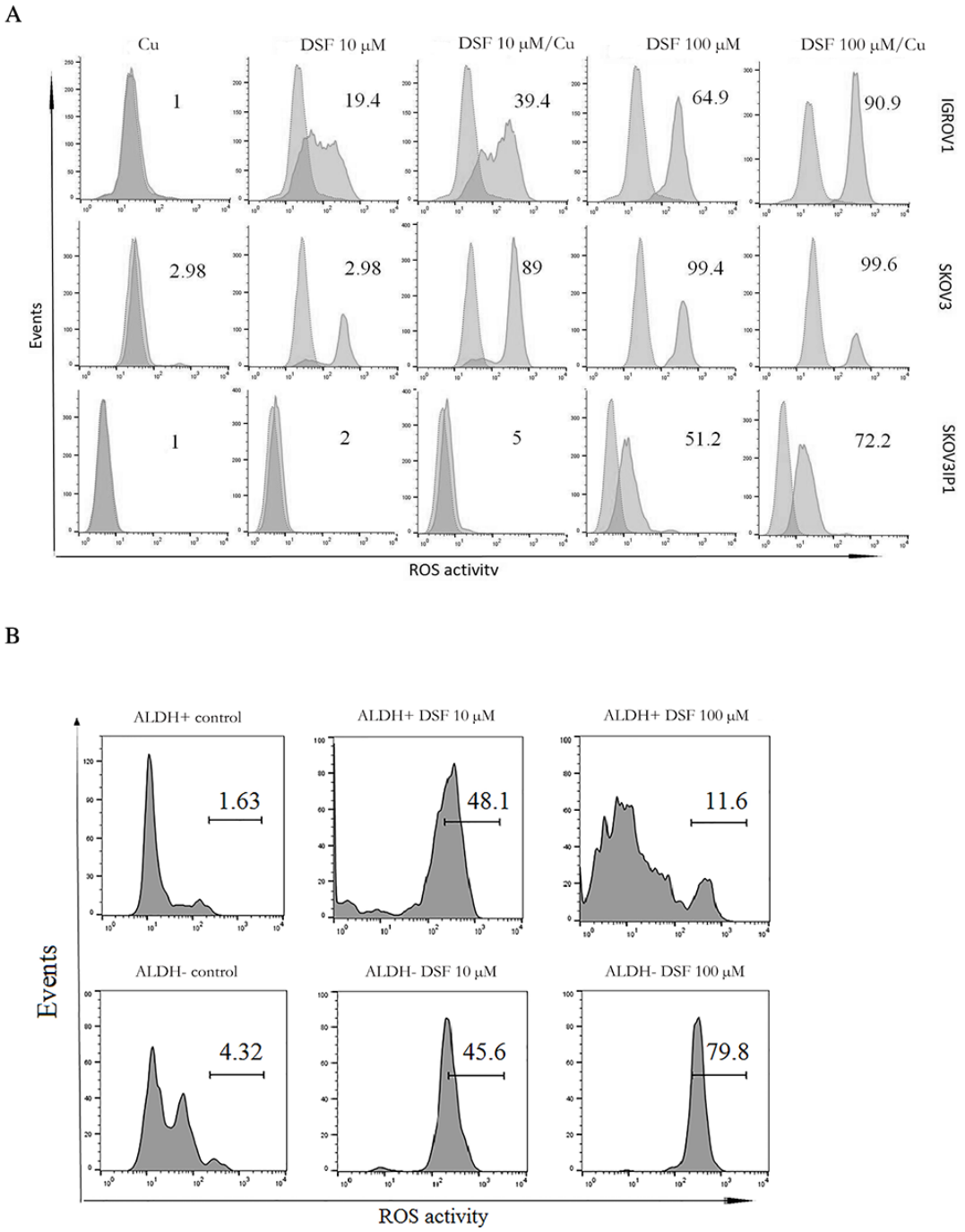

Figure 10: DSF/Cu^{2+} triggers ROS generation in ovarian cancer cell lines. A) Cancer cells were exposed to the indicated reagents and concentrations for 30 min followed by ROS assay. The dotted lines represent the untreated cells and the solid lines represent drug-treated cells, respectively. The relative ROS activity was calculated and normalized to untreated control cells. B) ALDH+ and ALDH- FACS-sorted cells from cell line SKOV3 were exposed to 10 µM DSF and 100 µM DSF. The relative ROS activity was gated. One representative of three independent experiments is shown.

5.9 DSF sensitizes cancer cells to cisplatin treatment

Although cisplatin has been used widely to treat cancers, tumors may develop an acquired resistance to cisplatin. One mechanism for cisplatin resistance is insufficient amount of cisplatin reaching the targeted DNA [93], which suggests that cisplatin-resistant cells decrease membrane transport of cisplatin and enhance cytoplasmic detoxification by increasing levels of thiol-containing species like glutathione (GSH) which has an important role in ROS elimination [94,95]. As DSF could react with thiol-containing molecules and decrease the level of GSH in cells [95], we investigated whether DSF could sensitize cancer cells to cisplatin treatment.

Cells were treated with 1 μM DSF, or 1 μM cisplatin, or 5 μM cisplatin, or combinations of DSF and cisplatin for 72 h, followed by MTT assay. As shown in Figure 11A, exposure to either DSF alone (1 μM) or cisplatin alone (1 μM) for 72 h only slightly reduced cell viability (by less than 10%), and exposure to cisplatin alone (5 μM) reduced the cell viability by less than 30%. However, a dramatic decrease of cell viability was induced by the drug combination with around 50% decrease in the 1 μM DSF /1 μM cisplatin combination, and around 80% decrease in 1 μM DSF /5 μM cisplatin combination in both SKOV3IP1 and IGROV1 cell lines.

We next examined the dose-response relationship for this potentiation by DSF. Different doses of DSF (0.3 μM, or 0.6 μM) were added to various concentrations of cisplatin (0.5 μM, 1 μM, 1.5 μM or 2 μM). The results indicated that DSF sensitized cancer cells to cisplatin treatment even at lower doses of 0.3 μM, with decreased cell viability of around 20% in both SKOV3IP1 and IGROV1 cell lines. Increased potentiation to sensitize the cells to cisplatin was observed at the higher dose of DSF at 0.6 μM (Figure 11B).

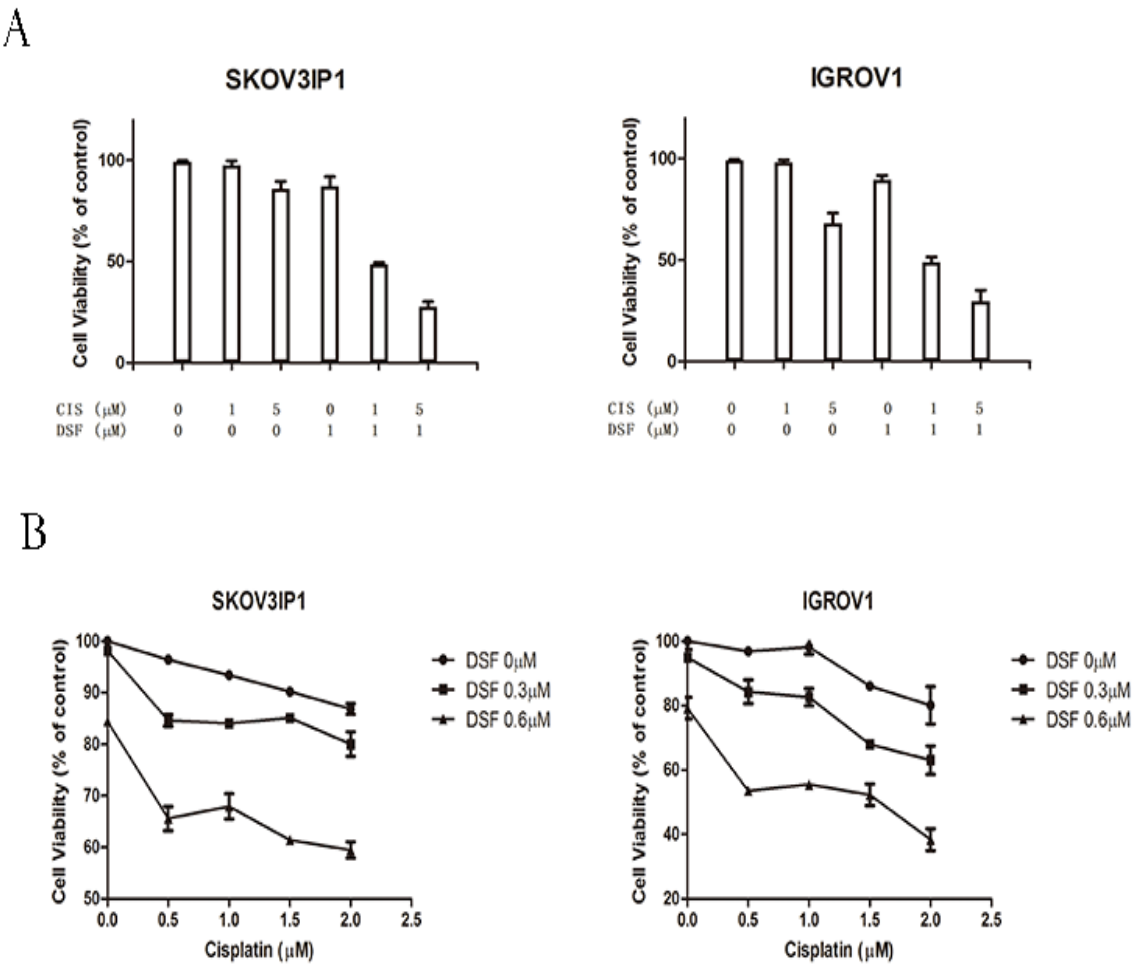

Figure 11: DSF sensitizes ovarian cancer cells to cisplatin treatment. A) SKOV3IP1 and IGROV1 cells were treated with either cisplatin alone (1 μM, 5 μM) or DSF alone (1 μM) or the indicated combinations for 72 h. B) IGROV1 and SKOV3IP1 cells were treated with the indicated concentrations of cisplatin, DSF and their combinations for 72 h. Cellular viability was detected by MTT assay. DSF, Disulfiram; Cis, cisplatin. All data presented are representative of three independent experiments.

5.10 DSF enhances cisplatin-induced cellular apoptosis

To further determine whether DSF sensitizes cisplatin treatment and suppresses cellular viability related to cellular apoptosis, we quantified the apoptotic status of cells after DSF/cisplatin treatment. We used flow cytometry with Annexin-V/PI staining after cells had been treated with DSF alone (1 μM), cisplatin alone (5 μM), and DSF (1 μM)/ cisplatin (5 μM) for 72 h. Cells cultured for 72 h without drug treatment were used as controls.

As shown in Figure 12, in the SKOV3IP1 cell line, early apoptosis was increased from 0.462% in control cells to 5.87% in cisplatin-only-treated cells, late apoptosis increased from 5.14% to 6.36%, and necrosis increased from 0.684% to 1.71%. However, a dramatic increase of cellular apoptosis and necrosis was induced when 1 μM DSF was combined with cisplatin, with early apoptosis, late apoptosis and necrosis increasing to 11.8%, 17.2%, and 4.88%, respectively. Similar results were observed in the IGROV1 cell line. Early apoptosis, late apoptosis and necrosis was increased from 25.3%, 21%, and 0.846% in cisplatin-only-treated cells to 35.7%, 35.3% and 1.02%, respectively, in DSF plus cisplatin-treated cells. DSF only (1 μM) treatment did not induce significantly more cellular apoptosis and necrosis compared to control cells. These results indicated that DSF enhanced cisplatin-induced cellular apoptosis in ovarian cancer cell lines.

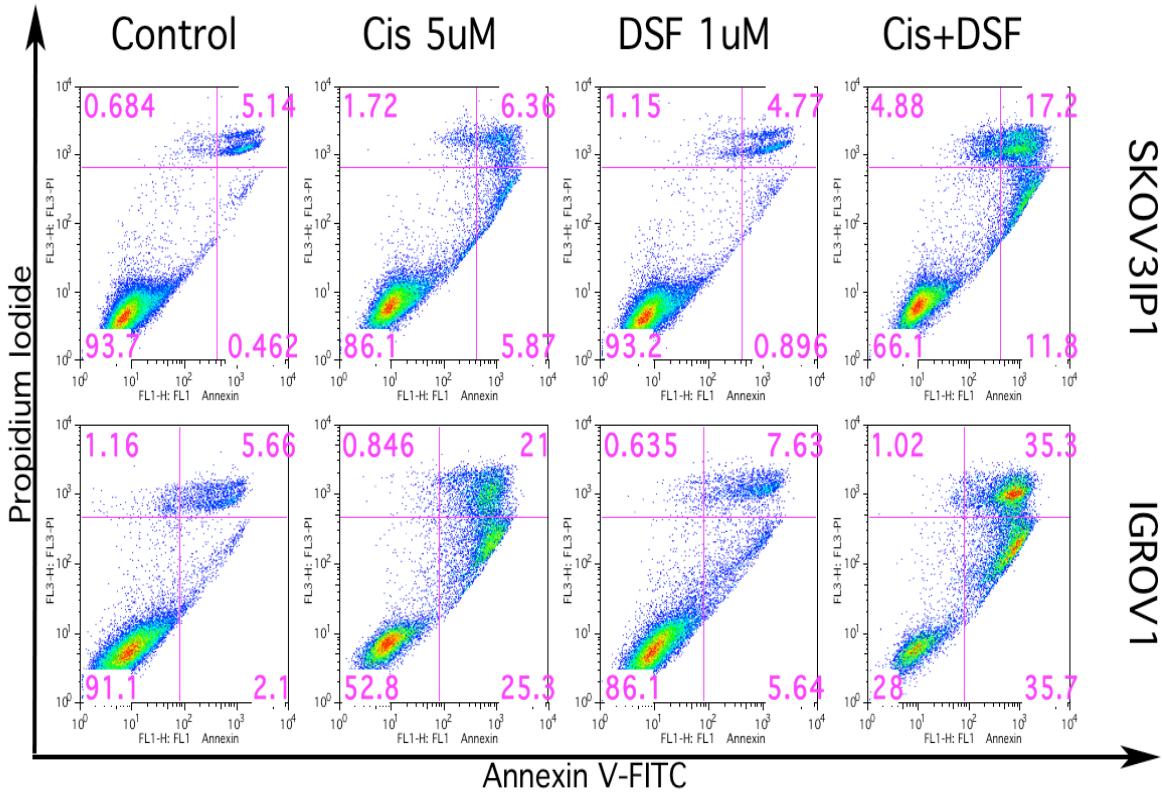

Figure 12: DSF enhances cisplatin-induced cellular apoptosis. Flow cytometric analysis exhibited the cellular apoptotic status. SKOV3IP1 and IGROV1 were treated with cisplatin (5 μM), DSF (1 μM) and their combination for 72 h. LL, LR, UR and UL are representative of live, early apoptotic, late apoptotic, and necrotic cells, separately. DSF, Disulfiram; Cis, cisplatin. All data presented are representative of three independent experiments.

5.11 Quantitative analysis of treatments with double and triple drug combination

To analyze the interference of different drugs used in this study, we have used a quantitative method to determine synergism or antagonism in treatments with two and three drug combinations in vitro. This method quantitatively measures the dose-effect relationship of each drug alone and its combinations and determines whether or not a given drug combination would result in a synergistic effect. The computer software allows automated simulation of synergism and antagonism at all dose or effect levels. Based on this algorithm, the combination index (CI) was used for quantitative determination of drug interactions, where CI < 1, 1, and > 1 indicate synergism, additive effect, and antagonism, respectively. The dose-reduction index (DRI) value is a measure of how many fold the dose of each drug in a synergistic combination may be reduced at a given effect level when compared with the doses of each drug alone.

The doses selected for each drug are described in the methods (see Table 1). All data were calculated by the CompuSyn program. The combination index (CI) and dose-reduction index (DRI) values at different effect levels are presented in Table 2 and Table 3. These values can be different at different effect levels. For the cisplatin and paclitaxel combination, there was a synergistic effect at broad effect level ranges from IC_{50} to IC_{90} in the IGROV1 cell line, while a slightly antagonistic effect was observed at IC_{90} level in the SKOV3IP1 cell line. However, cisplatin and DSF combination showed superior synergistic effects in both cell lines at broad effect level ranges from IC_{50} to IC_{90}, and this combination effect was even stronger than cisplatin combined with paclitaxel. For paclitaxel and DSF combination, the effect was quite different in different cell lines. There was a synergistic effect in the SKOV3IP1 cell line, while an antagonistic effect was observed in IGROV1. Finally, the combination of three drugs continued to yield a stronger synergistic effect in the SKOV3IP1 cell line since each two-drug combination was synergistic. In IGROV1 cell line, desirable synergistic effects were shown in three drug combinations, although there was antagonism between paclitaxel and DSF. Furthermore, due to the synergistic effect, the doses of each drug may be reduced by up to hundred-fold while maintaining an equal antitumor efficacy once they were in combinations. The combination of three drugs continued to yield desirable synergistic effects, while as expected DRI tended to be higher with three-drug combination than that in two-drug combinations.

Table 2: double and triple drug combination effect at 50%, 75%, and 95% inhibition of SKOV3IP1 cell growth.

A

Drug Combination	Combination Index at		
	IC50	IC75	IC90
Cis+Pac	0.104	0.267	3.170
Cis+DSF	0.123	0.176	0.311
Pac+DSF	1.021	0.048	0.004
Cis+Pac+DSF	0.286	0.110	0.196

B

Drug Combination		Dose-Reduction Index at		
		IC50	IC75	IC90
Cis+Pac	Cis	51.06	4.02	0.32
	Pac	11.89	54.81	252.58
Cis+DSF	Cis	11.74	4.80	1.97
	DSF	37.36	156.08	652.05
Pac+DSF	Pac	1.05	29.81	845.61
	DSF	14.36	70.96	350.68
Cis+Pac+DSF	Cis	49.80	5.39	1
	Pac	11.60	73.59	466.87
	DSF	158.48	175.17	193.61

A) Computer-simulated CI values for drug combinations at different levels of inhibition of SKOV3IP1 cell growth. B) Computer-simulated DRI values for drug combinations at different levels of inhibition of SKOV3IP1 cell growth. IC_{50}, IC_{75}, IC_{90} is the concentration required to inhibit cell growth by 50%, 75%, 90%, respectively. One representative of three independent experiments is shown.

Table 3: double and triple drug combination effect at 50%, 75%, and 95% inhibition of IGROV1 cell growth.

A

Drug Combination	Combination Index at		
	IC50	IC75	IC90
Cis+Pac	0.42	0.36	0.36
Cis+DSF	0.24	0.33	0.52
Pac+DSF	2.99	24.49	202.63
Cis+Pac+DSF	0.32	0.19	0.16

B

Drug Combination		Dose-Reduction Index at		
		IC50	IC75	IC90
Cis+Pac	Cis	3.50	3.23	2.97
	Pac	7.38	18.88	48.29
Cis+DSF	Cis	5.09	3.15	1.95
	DSF	25.38	57.17	128.76
Pac+DSF	Pac	0.47	0.05	0.006
	DSF	1.12	0.17	0.02
Cis+Pac+DSF	Cis	5.28	6.24	7.38
	Pac	11.12	36.49	119.78
	DSF	26.30	113.13	486.71

A) Computer-simulated CI values for drug combinations at different levels of inhibition of IGROV1 cell growth. B) Computer-simulated DRI values for drug combinations at different levels of inhibition of IGROV1 cell growth. IC_{50}, IC_{75}, IC_{90} is the concentration required to inhibit cell growth by 50%, 75%, 90%, respectively. One representative of three independent experiments is shown.

5.12 Experiments to verify calculated DRI values

To verify experimentally the DRI value in the combination effect calculated from double and triple drug combination data of the individual drug applications (Table 2, 3), the IC_{50} concentration of each drug was chosen, and compared to the reduced IC_{50} for the same drug combined with DSF. Thereby the synergistic effect was experimentally proven.

As shown in Figure 13A, for cell line SKOV3IP1, the $IC_{50\text{-cisplatin}}$ is at 22 μM; the $IC_{50\text{-paclitaxel}}$ is at 0.38 μM, and the combination of these two drugs at their original IC_{50} concentration without

DSF further increased cytotoxicity and reduced cellular viability by 20%. As shown in Table 2, the combination of cisplatin at a concentration of 0.4 μM, which is a reduction by 51.06-fold from 22 μM, with paclitaxel at 0.03 μM, which is a reduction by 11.89-fold from 0.38 μM, achieved the same cytotoxic effect with a cellular viability of around 50% (Figure 13A). In contrast, either cisplatin alone or paclitaxel alone at the reduced concentration by DRI calculation only slightly reduced the cellular viability. However, addition of DSF significantly enhanced the cytotoxicity of cisplatin and paclitaxel when $IC_{50\text{-}DSF}$ 20 μM was added. Importantly, the combination with DSF and low concentration of chemotherapeutic drugs reached almost the same cytotoxic effect of the original cisplatin + paclitaxel concentration without DSF (cell viability is around 20%). A similar effect was observed on cell line IGROV1 (Figure 13B). Combination of cisplatin at 0.68 μM which is a reduction by 3.5-fold from 2.4 μM, with paclitaxel at 0.06 μM which is a reduction by 7.4-fold from 0.46 μM induced the same cytotoxic effect as with cisplatin at 2.4 μM alone or paclitaxel at 0.46 μM alone. In conjunction with DSF-IC_{50} 3 μM, the combination yielded synergistic interactions with the conventional anti-tumor therapeutic drugs that had the strongest cytotoxic effect and reduced viability to 10%. This finding experimentally verified the previous observation that combination with DSF potentiates cytotoxicity, potentially improving a chemotherapeutic effect.

A

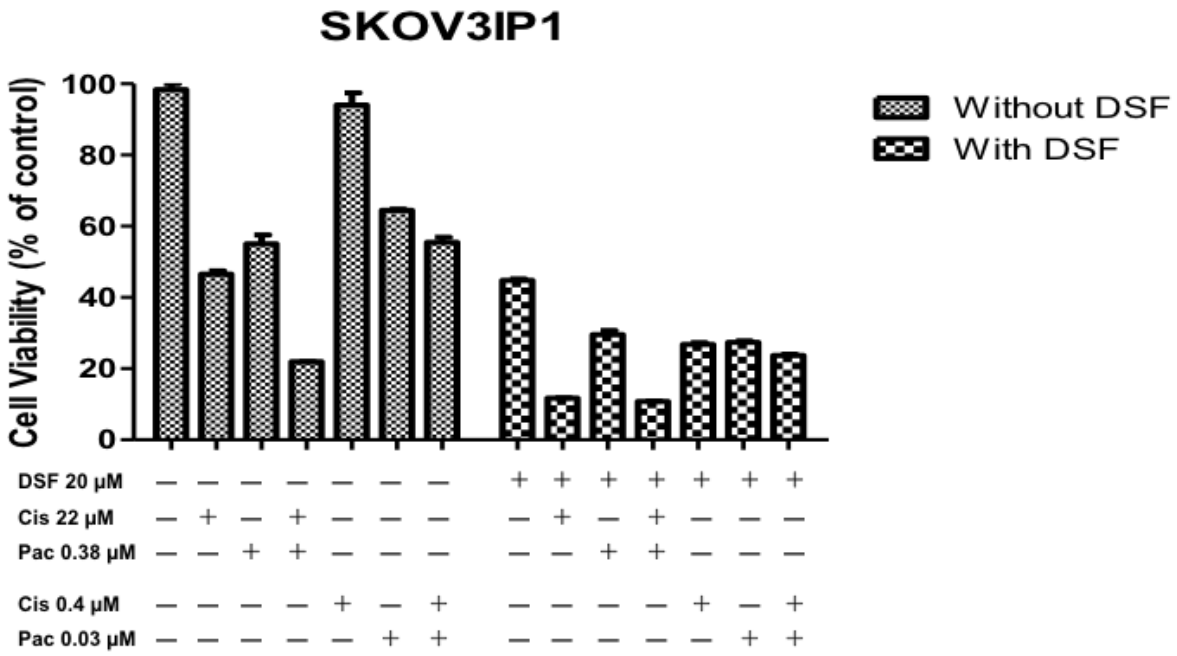

B

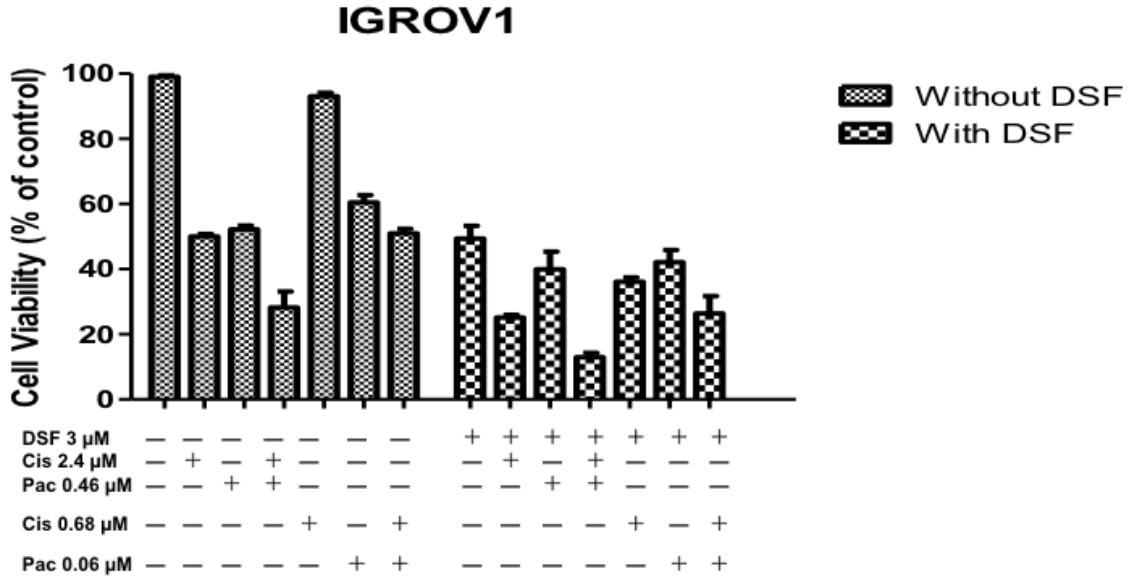

Figure 13: Experimental verification of calculated DRI values. SKOV3IP1 cells (A) and IGROV1 cells (B) were treated at indicated drug concentration or drug combination for 72 h. Cellular viability was detected by MTT assay. Untreated control cells were used as controls. One representative of three independent experiments is shown.

6 Discussion

Epithelial ovarian cancer (EOC) is the leading cause of gynecological cancer-related death [1], despite the high remission rate reaching 80%, most of the patients develop recurrence [96]. In recent decades, increasing evidence suggests that CSCs which are quiescent and slow-cycling cell populations with permanent differentiation and proliferative capacities, strong tumorigenicity, and high invasive and migratory abilities might be responsible for recurrence and metastasis of cancer [97]. Therefore, identification of drugs targeting CSCs as adjuvant treatment is urgently needed to improve the outcomes of ovarian cancer therapy.

The standard therapy in primary ovarian cancer is surgery followed by systemic chemotherapy with cisplatin plus paclitaxel. Unfortunately, ovarian cancer cells either intrinsically are or relatively rapidly become resistant to cisplatin-based chemotherapy, leading to relapse and therapeutic failure [1]. Another major problem besides cisplatin resistance is the greater toxicity of drug combinations. The main dose-limiting toxicity for cisplatin are nephrotoxicity, peripheral nerve toxicity and toxicity to the cochlea (inner ear toxicity) [97] due to the DNA damage induced by cisplatin. The dose-limiting toxicity of paclitaxel which binds to microtubules stabilizes them and suppresses normal cell division are hypersensitivity, neutropenia, and peripheral neuropathy [98,99]. Both drugs suppress cellular dynamics, leading to mitotic arrest and apoptosis in dividing cells. Their toxic effects are only partially overlapping. For enhanced treatment efficacy, efforts should be made to maximize cytotoxic effects of chemotherapeutic agents on tumor cells while minimizing their toxic effects on normal cells [100].

This study confirmed that disulfiram itself exhibits dose-dependent and time-dependent cytotoxicity in ovarian cancer cells. Exogenous Cu^{2+} is not necessary for the mechanism of action of DSF. However, the cytotoxicity of DSF was significantly enhanced by addition of Cu^{2+} in ovarian cancer cell lines. It was found that Cu^{2+} plays an important role in the biological pathways in the human body by activating some critical proteins such as superoxide dismutase, tyrosinase and cytochrome oxidase [101]; and the concentration of Cu^{2+} in cancerous tissues, such as breast, prostate, lung, and brain, is significantly higher than that of the normal tissues [102]. This may help to enable selective treatment with DSF in cancer cells with enhancement of cytotoxicity by the higher level of Cu^{2+} concentrations in cancers while sparing normal tissues. One scenario could be that lipophilic DSF penetrates into cancer cells and reacts with intracellular Cu^{2+} to form the DSF/Cu^{2+} complex (diethyldithio-carbomate (DDC)-Cu^{2+}) which is

more cytotoxic and induces cellular apoptosis [103]. Another scenario is that when exogenous Cu^{2+} is added into the medium, an instant and short-term action between DSF and Cu^{2+} happens, producing certain chemical species, such as ROS, which is toxic to cancer cells and causes instant cytotoxicity to cancer cells [104].

Next, we investigated the inhibitory effect of DSF on ALDH activity which is a well-accepted marker for CSCs. Elevated expression of ALDHs is not only related to enhanced tumorigenic and metastatic potential [105], but also related to chemotherapy resistance of cancer cells [106,107,108]. Landen Jr C.N. et al. have proven that ALDH+ ovarian cancer cells are resistant to a wide range of classical cytotoxic anticancer drugs. However, these cells can become resensitized to chemotherapy by ALDH silencing using nanoliposomal siRNA in ovarian cancer cell lines SKOV3TRip2 and A2780cp20 [105]. The current study demonstrated that DSF with or without Cu^{2+} supplementation significantly inhibited ALDH activity which is associated with many properties of ovarian cancer stem cells, such as spheroid formation, colony formation and chemotherapy resistance. Our present results also showed that DSF with or without Cu^{2+} significantly reduced the number of spheroids and reduced the clonogenic capacity of the tumor cells in all ovarian cancer cell lines investigated, indicating the inhibitory effect of DSF on CSCs on single cell level.

DSF inhibited ALDH activity. Studies have shown that ALDH acts as a ROS scavenger [109], and has the potential to decrease oxidative stress. Thereby, ALDH may protect stem cells against oxidative stress. We were interested in investigating the ROS generation after DSF treatment in ovarian cancer cells. The results showed that DSF significantly increased intracellular ROS levels in a dose-dependent manner and typically triggered cellular apoptosis. DSF combined with Cu^{2+} further enhanced the generation of ROS with higher levels of intracellular ROS than DSF treatment alone. Our data demonstrate that ROS which contributes to a wide variety of cell and tissue injury may have a key role in DSF/Cu^{2+}-induced cytotoxicity and apoptosis in ovarian cancer cell lines. DSF/Cu^{2+} inhibited ALDH activity which is generally a ROS scavenger, leading to a subsequent loss of ALDH-mediated protection against oxidative stress and finally triggering CSC apoptosis. Further, we compared the ROS levels in ALDH+ cells and ALDH- cells from SKOV3 cell line, and found that ROS levels are higher in ALDH- cells than ALDH+ cells. One explanation could be that ALDH- cancer cells need rapid growth, and have a higher demand for ATP due to metabolic processes, resulting in accumulation of intracellular ROS, while ALDH+ cells which display stem-like behaviors are quiescent and a slow-cycling cell

population with higher ALDH expression, thus enhanced ability to detoxify ROS. However, after DSF (10 μM) treatment, more ROS were generated in ALDH+ than in ALDH- cells due to the inhibition of ALDH which plays a significant role in cancer stem cells survival. When DSF concentration was increased to 100 μM, ROS levels decreased in ALDH+ cells. One explanation could be that ALDH+ cells were probably more vulnerable to DSF and were killed by this concentration.

All results above provide strong evidence that DSF, which modulates ALDH activity and ROS generation, and is enhanced by the addition of Cu^{2+}, could be a candidate as a novel adjuvant chemotherapeutic agent in ovarian cancer treatment. Moreover, DSF effectively suppressed ALDH activity and modulated ROS generation, leading us to conclude that DSF could combine with other conventional chemotherapy agents. To establish a new protocol designed to exploit both complementary and additive or synergistic effect, cytotoxicity of cisplatin and DSF combination was tested. We assessed the potential capability of DSF to combine with other chemotherapeutic agents in ovarian cancer treatment. We found that DSF could sensitize cisplatin treatment to cancer cells even at lower doses (0.3 μM), and significantly enhanced cisplatin-induced apoptosis in the cell lines investigated. Also, increased potentiation to sensitize cells to cisplatin treatment was observed at the higher dose of DSF at 0.6 μM. Flow cytometry results showed that early apoptosis, late apoptosis, and necrosis were all increased dramatically when cells were treated with DSF/cisplatin combination. These results indicated that DSF sensitizes cells to cisplatin treatment and suppresses cellular viability by inducing apoptosis in the cell lines investigated. Due to its chemo-sensitizing effects, DSF is very promising when used in combination with cisplatin-based chemotherapy to improve the therapeutic outcome. This is in agreement with the study of Wantong Song et al. study [93]. The fact that DSF modifies intracellular sulfhydryl groups could be one of the explanations. Most cisplatin-resistant tumor cells have increased intracellular sulfhydryl levels (mostly GSH). 75% to 80% of the activated platinum drugs are sequestered by the abundant GSH in cytoplasm, preventing cisplatin binding to DNA [110]. However, when DSF is combined with cisplatin, reduced GSH will react with DSF, the effectiveness of cisplatin is consequently improved [93].

Further, quantitative assessment of DSF combinations with cisplatin and paclitaxel was done in this study. The results showed that cisplatin and DSF combination yielded superior synergistic effects in the cell lines investigated at broad effect level ranges from IC_{50} to IC_{90}, and this synergistic effect was even stronger than cisplatin/paclitaxel combination. The effect of

paclitaxel/DSF combination, the effect was different in different cell lines. There was a synergistic effect in the SKOV3IP1 cell line, while in the IGROV1 cell line, the effect was antagonistic. Finally, the combination of three drugs continued to yield a superior synergistic effect in the SKOV3IP1 cell line as each of the two drugs was synergistic. In the IGROV1 cell line, desirable synergistic effects were shown in three drug combinations, although there was antagonism between paclitaxel and DSF. This DSF synergistic effect in multiple drug combinations may provide lots of therapeutic benefits in clinical treatment regimens against ovarian cancers. Firstly, it could increase or at least maintain the same efficacy but decrease the doses of each drug to reduce toxicity [91]. In our verification experiments, we found that relative cellular viability was around 20% when cells were treated with 22 μM cisplatin and 0.38 μM paclitaxel in the SKOV3IP1 cell line. However, in the presence of DSF, very low concentration of cisplatin at 0.4 μM which is a reduction by 51.06-fold from 22 μM, with paclitaxel at 0.03 μM which is a reduction by 11.89-fold from 0.38 μM reached almost the same cytotoxic effect as the original cisplatin + paclitaxel concentration without DSF. Similar results were observed in the IGROV1 cell line. Secondly, for cisplatin-resistant patients, DSF may increase the therapeutic efficacy by sensitizing cancer cells to cisplatin treatment [110]. Thirdly, it could minimize or slow down the development of drug resistance in patients. One explanation for this synergistic effect of DSF combined with cisplatin could be that DSF suppresses the outgrowth of the ALDH+ population which are therapy-resistant CSCs populations, modulating ROS generation, while conventional anticancer agents such as cisplatin target the disulfiram-insensitive, ALDH- population by modulating cell cycle or by other mechanisms. The result of the combination is that more cellular apoptosis is induced due to interaction of drugs exerting different toxic mechanisms.

In conclusion, although the cisplatin/paclitaxel combination has brought some benefits for ovarian cancer treatment, this regimen fails in many ovarian cancer patients due to the development of resistance to chemotherapy. In this in vitro model study, our findings support that DSF, which has a strong anti-tumor effect, inhibits ALDH activity, modulates ROS generation, and could be used as potential chemo-sensitizing agent to enhance the treatment efficacy of ovarian cancer cell lines. Due to its synergistic effect in combinations, the concentration of each chemotherapeutic agent may be reduced, thereby reducing the toxicity to normal tissues, while maintaining efficacy. Our present quantitative data analyses also provide evidence and strategies for a potential protocol design in clinical studies in the future. However, mechanisms of this synergistic effect still need further investigation, and more experiments are

also needed to further explore the effect of DSF on tissues from patients. For clinical trials, pharmacological limitations such as first-pass-effects have to be overcome.

7 References

1. Oronsky B, Ray CM, Spira AI, Trepel JB, Carter CA, Cottrill HM. A brief review of the management of platinum-resistant-platinum-refractory ovarian cancer. Med Oncol. 2017; 34: 103-110.

2. Wefers C, Lambert LJ, Torensma R, Hato SV. Cellular immunotherapy in ovarian cancer: targeting the stem of recurrence. Gynecol Oncol. 2015; 137: 335-342.

3. Vaughan S, Coward JI, Bast RC, Berchuck A, Berek JS, Brenton JD, Coukos G, Crum CC, Drapkin R, Etemadmoghadam D, Friedlander M, Gabra H, Kaye SB, Lard CJ, Lengyel E, Levine DA, McNeish IA, Menon U, Mills GB, Nephew KP, Oza AM, Sood AK, Stronach EA, Walczak H, Bowtell DD, Balkwill FR. Rethinking ovarian cancer: recommendations for improving outcomes. Nat Rev Cancer. 2011; 11: 719-725.

4. Schwab CL, English DP, Roque DM, Pasternak M, Santin AD. Past, present and future targets for immunotherapy in ovarian cancer. Immunotherapy. 2014; 6: 1279-1293.

5. Leitao MM, Chi DS. Surgical management of recurrent ovarian cancer. Semin Oncol. 2009; 36: 106-111.

6. Sehouli J, Grabowski JP. Surgery for recurrent ovarian cancer: Options and Limits. Best Pract Res Clin Obstet Gynaecol. 2016; 16: 30116:

7. Hennessy BT, Coleman RL, Markman M. Ovarian cancer. Lancet. 2009; 374:1371-1382.

8. P. Harter, A. du Bois. The role of surgery in ovarian cancer with special emphasis on cytoreductive surgery for recurrence. Curr Opin Oncol. 2005; 17: 505-514.

9. R.E.Bristow, I Puri, D.S.Chi. Cytoreductive surgery for recurrent ovarian cancer: a meta-analysis. Gynecol Oncol. 2009; 112: 265-274.

10. Parmar MK, Ledermann JA, Colombo N, du Bois A, Delaloye JF, Kristensen GB, Wheeler S, Swart AM, Qian W, Torri V, Floriani I, Jayson G, Lamont A, Tropé C. Paclitaxel plus platinum-based chemotherapy versus conventional platinum-based chemotherapy in women with relapsed ovarian cancer: the ICON4/AGO-OVAR-2.2 trial. Lancet. 2003; 361: 2099-2106.

11. Lloyd KL, Cree IA, Savage RS. Prediction of resistance to chemotherapy in ovarian cancer: A systematic review. BMC Cancer 2015; 15: 117.

12. Zheng ZG, Xu H, Suo SS, Xu XL, Ni MW, Gu LH, Chen W, Wang LY, Zhao Y, Tian B, Hua YJ. The essential role of H19 contributing to cisplatin resistance by regulating glutathione metabolism in high-grade serous ovarian cancer. Sci Rep. 2016; 6: 26093.

13. Galluzzi L, Senovilla L, Vitale I, Michels J, Martins I, Kepp O, Castedo M, Kroemer G. Molecular mechanisms of cisplatin resistance. Oncogene. 2012; 31:1869-1883.

14. Pacioni S, D'Alessandris QG, Giannetti S, Morgante L, De Pascalis I, Coccè V, Bonomi A, Pascucci L, Alessandri G, Pessina A, Falchetti ML, Pallini R. Mesenchymal stromal cells loaded with paclitaxel induce cytotoxic damage in glioblastoma brain xenografts. Stem Cell Res Ther. 2015; 6: 194.
15. Gornstein E. Schwarz TL. The paradox of paclitaxel neurotoxicity: mechanisms and unanswered questions. Neuropharmacology. 2014; 76: 175-183.
16. Tambe M, Pruikkonen S, Mäki-Jouppila J, Chen P, Elgaaen BV, Straume AH, Huhtinen K, Cárpen O, Lønning PE, Davidson B, Hautaniemi S, Kallio MJ. Novel Mad2-targeting miR-493-3p controls mitotic fidelity and cancer cells' sensitivity to paclitaxel. Oncotarget. 2016; 7: 12267-12285.
17. Bergmann TK, Brasch-Andersen C, Gréen H, Mirza MR, Skougaard K, Wihl J, Keldsen N, Damkier P, Peterson C, Vach W, Brøsen K. Impact of ABCB1 variants on neutrophil depression: a pharmacogenomics study of paclitaxel in 92 women with ovarian cancer. Basis Clin Pharmacol Toxicol. 2012; 110: 199-204.
18. Lapidot T, Sirard C, Vormoor J, Murdoch B, Hoang T, Caceres-Cortes J, Minden M, Paterson B, Caligiuri MA, Dick JE. A cell initiating human acute myeloid leukaemia after transplantation into SCID mice. Nature. 1994; 367: 645-648.
19. Foster R, Buckanovich RJ, Rueda BR. Ovarian cancer stem cells: Working towards the root of stemness. Cancer Lett. 2013; 338: 147-157.
20. Magee JA, Piskounova E, Morrison SJ. Cancer stem cells: impact, heterogeneity, and uncertainty. Cancer Cell. 2012; 21: 283-196.
21. Friedmann-Morvinski D, Verma IM. Dedifferentiation and reprogramming: origins of cancer stem cells. EMBO Rep. 2014; 15: 244-253.
22. Ricci-Vitiani L, Fabrizi E, Palio E, De Maria R. Colon cancer stem cells. J Mol Med. 2009; 87: 1097-1104.
23. Ghods AJ, Irvin D, Liu G, Yuan X, Abdulkadir IR, Tunici P Konda B, Wachsmann-Hogiu S, Black KL, Yu JS. Spheres isolated from 9L gliosarcoma rat cell line possess chemoresistant and aggressive cancer stem-like cells. Stem Cells. 2007; 25: 1645-1653.
24. Fang D, Nguyen TK, Leishear K, Finko R, Kulp AN, Hotz S, Van Belle PA, Xu X, Elder DE, Herlyn M. A tumorigenic subpopulation with stem cell properties in melanomas. Cancer Res. 2005; 65: 9328-9337.
25. Ponti D, Costa A, Zaffaroni N, Pratesi G, Petrangolini G, Coradini D, Pilotti S, Pierotti MA, Daidone MG. Isolation and in vitro propagation of tumorigenic breast cancer cells with stem/progenitor cell properties. Cancer Res. 2005; 65: 5506-5511.

26. Chen C, Wei Y, Hummel M, Hoffmann TK, Gross M, Kaufmann AM, Albers AE. Evidence for epithelial-mesenchymal transition in cancer stem cells of head and necksquamous cell carcinoma. Plos One. 2011: e16466.
27. Bapat SA, Mali AM, Koppikar CB, Kurrey NK. Stem and progenitor-like cells contribute to the aggressive behavior of human epithelial ovarian cancer. Cancer Res. 2005; 65:3025-3029.
28. Reya T, Morrison SJ, Clarke MF, Weissman IL. Stem cells, cancer, and cancer stem cells. Nature. 2001; 414: 105-111.
29. Monjri M. Shah, Charles N. Landen. Ovarian cancer stem cells: Are They Real and Why are they Important? Gynecol Oncol. 2014; 132: 483-489.
30. Bowen NJ, Walker LD, Matyunina LV, Logani S, Totten KA, Benigno BB, McDonald JF. Gene expression profiling supports the hypothesis that human ovarian surface epithelia are multipotent and capable of serving as ovarian cancer initiating cells. BMC medical genomics. 2009; 2: 71.
31. Wang Y, Li W, Patel SS, Cong J, Zhang N, Sabbatino F, Liu X, Qi Y, Huang P, Lee H, Taghian A, Li JJ, DeLeo AB, Ferrone S, Epperly MW, Ferrone CR, Ly A, Brachtel EF, Wang X. Blocking the formation of radiation-induced breast cancer stem cells. Oncotarget. 2014; 5: 3743-3755.
32. Tomita H, Tanaka K, Tanaka T, Hara A. Aldehyde dehydrogenase 1A1 in stem cells and cancer. Oncotarget. 2016; 7: 11018-11032.
33. Chen Y, Thompson DC, Koppaka V, Jester JV, and Vasiliou V. Ocular aldehyde dehydrogenases: protection against ultraviolet damage and maintenance of transparency for vision. Prog Retin Eye Res. 2013; 33: 28-39.
34. Rodriguez-Torres M, Allan AL. Aldehyde dehydrogenase as a marker and functional mediator of metastasis in solid tumors. Clin Exp Metastasis. 2016; 33: 97-113.
35. Ying M, Wang S, Sang Y, Sun P, Lal B, Goodwin CR, Guerrero-Cazares H, Quinones-Hinojosa A, Laterra J, and Xia S. Regulation of glioblastoma stem cells by retinoic acid: role for Notch pathway inhibition. Oncogene. 2011; 30: 3454-3467.
36. Chanda B, Ditadi A, Iscove NN, and Keller G. Retinoic acid signaling is essential for embryonic hematopoietic stem cell development. Cell. 2013; 155: 215-227.
37. Qiu JJ, Zeisig BB, Li S, Liu W, Chu H, Song Y, Giordano A, Schwaller J, Gronemeyer H, Dong S, and So CW. Critical role of retinoid/rexinoid signaling in mediating transformation and therapeutic response of NUP98-RARG leukemia. Leukemia. 2015; 29: 1153-1162.
38. Huang EH, Hynes MJ, Zhang T, Ginestier C, Dontu G, Appelman H, Fields JZ, Wicha MS, Boman BM. Aldehyde Dehydrogenase 1 Is a Marker for Normal and Malignant Human Colonic

Stem Cells (SC) and Tracks SC Overpopulation during Colon Tumorigenesis. Cancer Research. 2009; 69: 3382-3389.
39. Singh S, Brocker C, Koppaka V, Chen Y, Jackson BC, Matsumoto A, Thompson DC, Vasiliou V. Aldehyde dehydrogenases in cellular responses to oxidative/electrophilicstress. Free Radical Biology and Medicine. 2013; 56: 89-101.
40. Xu X, Chai S, Wang P, Zhang C, Yang Y, Yang Y, and Wang K. Aldehyde dehydrogenases and cancer stem cells. Cancer Lett. 2015; 369: 50-57.
41. Liu S, Cong Y, Wang D, Sun Y, Deng L, Liu Y, Martin-Trevino R, Shang L, McDermott SP, Landis MD, Hong S, Adams A, D'Angelo R, Ginestier C, Charafe-Jauffret E, Clouthier SG, Birnbaum D, Wong ST, Zhan M, Chang JC, Wicha MS. Breast cancer stem cells transition between epithelial and mesenchymal states reflective of their normal counterparts. Stem Cell Rep.2014; 2: 78-91.
42. Liao J, Qian F, Tchabo N, Mhawech-Fauceglia P, Beck A, Qian Z, Wang X, Huss WJ, Lele SB, Morrison CD. Ovarian cancer spheroid cells with stem cell-like properties contribute to tumor generation, metastasis and chemotherapy resistance through hypoxia-resistant metabolism. PLoS One. 2014;9: e84941.
43. Kuroda T, Hirohashi Y, Torigoe T, Yasuda K, Takahashi A, Asanuma H, Morita R, Mariya T, Asano T, Mizuuchi M, Saito T, Sato N: ALDH1-high ovarian cancer stem-like cells can be isolated from serous and clear cell adenocarcinoma cells, and ALDH1 high expression is associated with poor prognosis. PLoS One. 2016; 8: e65158.
44. Mu X, Isaac C, Greco N, Huard J, Weiss K. Notch signaling is associated with ALDH activity and an aggressive metastatic phenotype in murine osteosarcoma cells. Front Oncol. 2013; 3: 143.
45. van den Hoogen C, van der Horst G, Cheung H, Buijs JT, Pelger RC, van der Pluijm G. The aldehyde dehydrogenase enzyme 7A1 is functionally involved in prostate cancer bone metastasis. Clin Exp Metastasis.2011; 28: 615-625.
46. Ajani J, Wang X, Song S, Suzuki A, Taketa T, Sudo K, Wadhwa R, Hofstetter W, Komaki R, Maru D. ALDH-1 expression levels predict response or resistance to preoperative chemoradiation in resectable esophageal cancer patients. Mol Oncol. 2014;8: 142-149.
47. Charafe-Jauffret E, Ginestier C, Bertucci F, Cabaud O, Wicinski J, Finetti P, Josselin E, Adelaide J, Nguyen T-T, Monville F. ALDH1-positive cancer stem cells predict engraftment of primary breast tumors and are governed by a common stem cell program. Cancer Res. 2013; 73: 7290-7300.

48. Condello S, Morgan C, Nagdas S, Cao L, Turek J, Hurley T, Matei D. b-Catenin-regulated ALDH1A1 is a target in ovarian cancer spheroids. Oncogene. 2015; 34: 2297-2308.
49. Choi SA, Lee JY, Phi JH, Wang K-C, Park C-K, Park S-H, Kim S-K. Identification of brain tumour initiating cells using the stem cell marker aldehyde dehydrogenase. Eur J Cancer. 2014; 50: 137-149.
50. Liang D, Shi Y. Aldehyde dehydrogenase-1 is a specific marker for stem cells in human lung adenocarcinoma. Med Oncol. 2012; 29: 633-639.
51. Lin J, Liu X, Ding D. Evidence for epithelial-mesenchymal transition in cancer stem-like cells derived from carcinoma cell lines of the cervix uteri. Int J Clin Exper Pathol. 2015; 8: 847.
52. Triscott J, Rose Pambid M, Dunn SE. Concise review: bullseye: targeting cancer stem cells to improve the treatment of gliomas by repurposing disulfiram. Stem Cell. 2015; 33: 1042-1046.
53. Hald J, Jacobsen E. A drug sensitizing the organism to ethyl alcohol. Lancet 1948; 2: 1001-1004.
54. Sen, C.K. and Packer, L. Thiol homeostasis and supplements in physical exercise. Am. J. Clin. Nutr. 2000; 72, 653S-669S.
55. Requejo R, Hurd TR, Costa NJ, Murphy MP. Cysteine residues exposed on protein surfaces are the dominant intramitochondral thiol and may protect against oxidative damage. FEBS J. 2010; 277: 1465-1480.
56. Gregoriadis GC, Apostolidis NS, Romanos AN, Paradellis TP. A comparative study of trace elements in normal and cancerous colorectal tissues. Cancer. 1983; 52: 508-519.
57. Wang F, Zhai S, Liu X, Li L, Wu S, Dou QP, Yan B. A novel dithiocarbamate analogue with potentially decreased ALDH inhibition has copper-dependent proteasome-inhibitory and apoptosis-inducing activity in human breast cancer cells. Cancer Letters. 2011; 300: 87-95.
58. Iljin K, Ketola K, Vainio P, Halonen P, Kohonen P, Fey V, Grafstrom RC, Perala M, Kallioniemi O. High-Throughput Cell-Based Screening of 4910 Known Drugs and Drug-like Small Molecules Identifies Disulfiram as an Inhibitor of Prostate Cancer Cell Growth. Clinical Cancer Research. 2009; 15: 6070-6078.
59. Guo X, Xu B, Pandey S, Goessl E, Brown J, Armesilla AL, Darling JL, Wang W. Disulfiram/copper complex inhibiting NFκB activity and potentiating cytotoxic effect of gemcitabine on colon and breast cancer cell lines. Cancer Letters. 2010; 290: 104-113.
60. Yip NC, Fombon IS, Liu P, Brown S, Kannappan V, Armesilla AL, Xu B, Cassidy J, Darling JL, Wang W. Disulfiram modulated ROS–MAPK and NFκB pathways and targeted breast cancer cells with cancer stem cell-like properties. British Journal of Cancer. 2011; 104: 1564-1574.

61. Conticello C, Martinetti D, Adamo L, Buccheri S, Giuffrida R, Parrinello N, Lombardo L, Anastasi G, Amato G, Cavalli M, Chiarenza A, De Maria R, Giustolisi R, Gulisano M, Di Raimondo F. Disulfiram, an old drug with new potential therapeutic uses for human hematological malignancies. Int J Cancer. 2012; 131: 2197-2203.
62. Gorrini C, Harris IS, Mak TW. Modulation of oxidative stress as an anticancer strategy. Nature review. 2014; 12:931-947.
63. Irani, K, Xia Y, Zweier JL, Sollott SJ, Der CJ, Fearon ER, Sundaresan M, Finkel T, Goldschmidt-Clermont PJ. Mitogenic signaling mediated by oxidants in Ras-transformed fibroblasts. Science.1997; 275: 1649-1652.
64. Kincaid MM, Cooper AA. ERADicate ER stress or die trying. Antioxid. Redox Signal.2007; 9: 2373-2387.
65. Bell EL, Chandel NS. Mitochondrial oxygen sensing: regulation of hypoxia-inducible factor by mitochondrial generated reactive oxygen species. Essays Biochem.2007; 43: 17-27.
66. Semenza GL. Oxygen sensing, homeostasis, and disease. N. Engl. J. Med. 2011, 365: 537-547.
67. Meister A. Glutathione deficiency produced by inhibition of its synthesis, and its reversal; applications in research and therapy. Pharmacol. Ther. 1991; 51: 155-194.
68. Vurusaner B, Poli G, Basaga H. Tumor suppressor genes and ROS: complex networks of interactions. Free Radic. Biol. Med.2012; 52: 7-18.
69. Vousden KH, Ryan KM. p53 and metabolism. Nature Rev. Cancer. 2009; 9: 691-700.
70. Bouayed J, Bohn T. Exogenous antioxidants-double-edged swords in cellular redox state: health beneficial effects at physiologic doses versus deleterious effects at high doses. Oxid. Med. Cell Longev. 2010; 3: 228-237.
71. Janssen-Heininger YM, Mossman BT, Heintz NH, Forman HJ, Kalyanaraman B, Finkel T, Stamler JS, Rhee SG, van der Vliet A. Redox-based regulation of signal transduction: principles, pitfalls, and promises. Free Radic. Biol. Med. 2008; 45: 1-17.
72. Rhee SG. H_2O_2, a necessary evil for cell signaling. Science. 2006; 312: 1882-1883.
73. Perry G, Raina AK, Nunomura A, Wataya T, Sayre LM, Smith MA. How important is oxidative damage? Lessons from Alzheimer's disease. Free Radic Biol. Med. 2000; 28: 831-834.
74. Patel BP, Rawal UM, Dave TK, Rawal RM, Shukla SN, Shah PM, Patel PS. Lipid peroxidation, total antioxidant status, and total thiol levels predict overall survival in patients with oral squamous cell carcinoma. Integr. Cancer Ther. 2007; 6: 365-372.
75. Tsao SM, Yin MC, Liu WH. Oxidant stress and B vitamins status in patients with non-small cell lung cancer. Nutr. Cancer. 2007; 59: 8-13.

76. Zhou Y, Hileman EO, Plunkett W, Keating MJ, Huang P. Free radical stress in chronic lymphocytic leukemia cells and its role in cellular sensitivity to ROS generating anticancer agents. Blood. 2003; 101: 4098-4104.
77. Trachootham D, Alexandre J, and Huang P. Targeting cancer cells by ROS-mediated mechanisms: a radical therapeutic approach? Nat Rev Drug Discov.2009; 8: 579-591.
78. Rodrigues MS, Reddy MM, Sattler M. Cell cycle regulation by oncogenic tyrosine kinases in myeloid neoplasias: from molecular redox mechanisms to health implications. Antioxid. Redox Signal.2008; 10: 1813-1848.
79. Brandon M, Baldi P, Wallace DC. Mitochondrial mutations in cancer. Oncogene. 2006; 25: 4647-4662.
80. Horn HF, Vousden KH. Coping with stress: multiple ways to activate p53. Oncogene. 2007; 26: 1306-1316.
81. Azad N, Rojanasakul Y, Vallyathan V. Inflammation and lung cancer: roles of reactive oxygen/nitrogen species. J. Toxicol. Environ. Health B Crit. Rev. 2008; 11: 1-15.
82. Cook, JA, Gius D, Wink DA, Krishna MC, Russo A, Mitchell JB. Oxidative stress, redox, and the tumor microenvironment. Semin. Radiat. Oncol. 2004; 14: 259-266.
83. Tsatmali M, Walcott EC, Crossin KL. Newborn neurons acquire high levels of reactive oxygen species and increased mitochondrial proteins upon differentiation from progenitors. Brain Res. 2005; 1040: 137-50.
84. Ito K, Hirao A, Arai F, Matsuoka S, Takubo K, Hamaquchi I, Nomiyama K, Hosokawa K, Sakurada K, Nakaqata N, Ikeda Y, Mak TW, Suda T. Regulation of oxidative stress by ATM is required for self-renewal of haematopoietic stem cells. Nature. 2004; 431: 997-1002.
85. Tothova Z, Kollipara R, Huntly BJ, Lee BH, Castrillon DH, Cullen DE, McDowell EP, Lazo-Kallanian S, Williams IR, Sears C, Armstrongs SA, Passeque E, DePinho RA, Gilliland DG. FoxOs are critical mediators of hematopoietic stem cell resistance to physiologic oxidative stress. Cell. 2007; 128: 325-39.
86. Diehn M, Cho RW, Lobo NA, Kalisky T, Dorie MJ, Kulp AN, Qian D, Lam JS, Ailles LE, Wong M, Joshua B, Kaplan MJ Wapnir I, Dirbas FM, Somlo G, Garberoglio C, Paz B, Shen J, Lau SK, Quake SR, Brown JM, Weissman IL, Clarke MF. Association of reactive oxygen species levels and radioresistance in cancer stem cells. Nature. 2009; 458: 780-783.
87. Singh S, Brocker C, Koppaka V, Chen Y, Jackson BC, Matsumoto A, Thompson DC, Vasiliou V. Aldehyde dehydrogenases in cellular responses to oxidative/electrophilicstress. Free Radical Biology and Medicine. 2013; 56: 89-101.

88. Requejo R, Hurd TR, Costa NJ, Murphy MP. Cysteine residues exposed on protein surfaces are the dominant intramitochondrial thiol and may protect against oxidative damage. FEBS J. 2010; 277: 1465-1480.
89. Farnie G, Sotgia F, Lisanti MP. High mitochondrial mass identifies a sub-population of stem-like cancer cells that are chemo-resistant. Oncotarget. 2015; 6: 30472-30486.
90. Mauricio Rodriguez-Torres, Alison L. Allan. Aldehyde dehydrogenase as a marker and functional mediator of metastasis in solid tumors. Clin Exp Metastasis. 2016; 33: 97-113.
91. Chou TC, Motzer RJ, Tong Y, Bosl GJ. Computerized quantitation of synergism and antagonism of taxol, topotecan, and cisplatin against human teratocarcinoma cell growth: a rational approach to clinical protocol design. J Natl Cancer Inst. 1994; 86: 1517-1524.
92. Chou TC, Talalay P. Quantitative analysis of dose-effect relationships: The combined effects of multiple drugs or enzyme inhibitors. Adv Enzyme Regul. 1984; 22: 27-55.
93. Song W, Tang Z, Shen N, Yu H, Jia Y, Zhang D, Jiang J, He C, Tian H, Chen X. Combining disulfiram and poly (l-glutamic acid)-cisplatin conjugates for combating cisplatin resistance. J Control Release. 2016; 231: 94-102.
94. Mistry P, Kelland LR, Abel G, Sidhar S, Harrap KR. The relationships between glutathione, glutathione-S-transferase and cytotoxicity of platinum drugs and melphalan in 8 human ovarian-carcinoma cell-lines. Br. J. Cancer.1991; 64: 215-220.
95. Godwin AK, Meister A, Odwyer PJ, Huang CS, Hamilton TC, Anderson ME. High-resistance to cisplatin in human ovarian-cancer cell-lines is associated with marked increase of glutathione synthesis. Proc. Natl. Acad. Sci. 1992; 89: 3070-3074.
96. Heintz AP, Odicino F, Maisonneuve P, Quinn MA, Benedet JL, Creasman WT, Ngan HY, Pecorelli S, Beller U. Carcinoma of ovary. FIGO 26th Annual Report on the Results of Treatment in Gynecological Cancer. Int J Gynaecol Obstet. 2006; 95: 161-192.
97. Galluzzi L, Senovilla L, Vitale I, Michels J, Martins I, Kepp O, Castedo M, Kroemer G. Molecular mechanisms of cisplatin resistance. Oncogene. 2012; 31:1869-1883.
98. Tambe M, Pruikkonen S, Mäki-Jouppila J, Chen P, Elgaaen BV, Straume AH, Huhtinen K, Cárpen O, Lønning PE, Davidson B, Hautaniemi S, Kallio MJ. Novel Mad2-targeting miR-493-3p controls mitotic fidelity and cancer cells' sensitivity to paclitaxel. Oncotarget. 2016; 7: 12267-12285.
99. Parmar MK, Ledermann JA, Colombo N, du Bois A, Delaloye JF, Kristensen GB, Wheeler S, Swart AM, Qian W, Torri V, Floriani I, Jayson G, Lamont A, Tropé C. Paclitaxel plus platinum-based chemotherapy versus conventional platinum-based chemotherapy in women with relapsed ovarian cancer: the ICON4/AGO-OVAR-2.2 trial. Lancet. 2003; 361: 2099-2106.

100. Amini A, Masoumi-Moghaddam S, Ehteda A, Liauw W, Morris DL. Potentiation of chemotherapeutics by bromelain and N-acetylcysteine: sequential and combination therapy of gastrointestinal cancer cells. Am J Cancer Res. 2016; 6: 350-369.
101. Hogarth G. Metal-dithiocarbamate complexes: chemistry and biological activity. Mini Rev Med Chem. 2012; 12: 1202-1215.
102. Gregoriadis GC, Apostolidis NS, Romanos AN, Paradellis TP. A comparative study of trace elements in normal and cancerous colorectal tissues. Cancer. 1983; 52: 508-519.
103. Papaioannou M, Mylonas I, Kast RE, Brüning A. Disulfiram/copper causes redox-related proteotoxicity and concomitant heat shock response in ovarian cancer cells that is augmented by auranofin-mediated thioredoxin inhibition. Oncoscience. 2013;1: 21-29.
104. Tawari PE, Wang Z, Najlah M, Tsang CW, Kannappan V, Liu P, McConville C, He B, Armesilla AL, Wang W. The cytotoxic mechanisms of dislfiram and copper (II) in cancer cells. Toxicol Res. 2015; 4: 1439-1442.
105. Landen CN, Goodman B, Katre AA, Steg AD, Nick AM, Stone RL, Miller LD, Mejia PV, Jennings NB, Gershenson DM, Bast RC, Coleman RL, Lopez-Berestein G, Sood AK. Targeting Aldehyde Dehydrogenase Cancer Stem Cells in Ovarian Cancer. Molecular Cancer Therapeutics. 2010; 9: 3186-3199.
106. Sládek N, Kollander R, Sreerama L, Kiang D. Cellular levels of aldehyde dehydrogenases (ALDH1A1 and ALDH3A1) as predictors of therapeutic responses to cyclophosphamide-based chemotherapy of breast cancer: a retrospective study. Cancer Chemotherapy and Pharmacology. 2002; 49: 309-321.
107. Chang B, Liu G, Xue F, Rosen DG, Xiao L, Wang X, Liu J. ALDH1 expression correlates with favorable prognosis in ovarian cancers. Modern Pathology. 2009; 22: 817-823.
108. Huang K, Li LA, Meng YG, You YQ, Fu XY, Song L. Arctigenin Promotes Apoptosis in Ovarian Cancer Cells via the iNOS/NO/STAT3/Survivin Signalling. Basic Clin Pharmacol Toxicol. 2014; 115: 507-511.
109. Singh S, Brocker C, Koppaka V, Chen Y, Jackson BC, Matsumoto A, Thompson DC, Vasiliou V. Aldehyde dehydrogenases in cellular responses to oxidative/electrophilicstress. Free Radical Biology and Medicine. 2013; 56: 89-101.
110. Chen HHW, Song IS, Hossain A, Choi MK, Yamane Y, Liang ZD, Lu J, Wu LY, Siddik ZH, Klomp LW, Savaraj N, Kuo MT. Elevated glutathione levels confer cellular sensitization to cisplatin toxicity by upregulation of copper transporter hCtr1. Mol Pharmacol. 2008; 74: 697-704.

8 Curriculum Vita

My curriculum vitae does not appear in the electronic version of my paper for reasons of data protection.

9 Affidavit

“I, [Fang, Guo] certify under penalty of perjury by my own signature that I have submitted the thesis on the topic [Characterization of cytotoxic effect by disulfiram in ovarian cancer cell lines] I wrote this thesis independently and without assistance from third parties, I used no other aids than the listed sources and resources.

All points based literally or in spirit on publications or presentations of other authors are, as such, in proper citations (see "uniform requirements for manuscripts (URM)" the ICMJE www.icmje.org) indicated. The sections on methodology (in particular practical work, laboratory requirements, statistical processing) and results (in particular images, graphics and tables) correspond to the URM (s.o) and are answered by me. My interest in any publications to this dissertation correspond to those that are specified in the following joint declaration with the responsible person and supervisor. All publications resulting from this thesis and which I am author correspond to the URM (see above) and I am solely responsible.

The importance of this affidavit and the criminal consequences of a false affidavit (section 156,161 of the Criminal Code) are known to me and I understand the rights and responsibilities stated therein.

Date Signature

10 Acknowledgements

I would like to express my sincere gratitude to my supervisor Dr. Andreas M. Kaufmann, for offering the precious opportunity to study at Charité-Universitätsmedizin Berlin, Campus Benjamin Franklin, for the patient guidance, kind encouragement and continuous support throughout the entire period of my study. I feel extremely lucky and thankful that I met such a nice supervisor in my life, who cared so much about my work as well as my personal life, and who had confidence in me and encouraged me all the time. Experiments were always full of difficulties and troubles, however, each time I hovered between adhering to and giving up, I could always get encouragement and support from him. His support and guidance, even his smile will always be appreciated and remembered lifelong.

I would also like to express my sincere gratitude to Dr. Andreas Albers, who always provided me with professional ideas and suggestions, who always found time to talk with us and cared about the progress of the experiments. Discussing with him every time helped me with a lot of constructive directions.

I am very grateful to Jinfeng Xu who acted like my teacher as well as brother in the lab, he really taught me quite a lot with patience, from experiment techniques to theories, I could always make progress in my experiments due to his enthusiastic help. I am indebted to him for his help.

I would also like to thank all the other members in the lab, Dana Schiller, Tina Kube, Amrei Krings, Sarina Sarina, Wenhao Yao, Zhifeng Sun, Weiming Hu, Aleksandra Pesic, Mirka Basten, Nora Franziska Nevermann, Sarah-Maria Klaes, and so on. I have much appreciation for all of you, the friendship with you is a treasure to me for all my life, and the happy time with you made my world full and bright.

I own my sincere gratitude to my parents and my friends for your love, encouragement and support in every step on my way. I believe that wherever I go, whatever I do, they will all be backing me, supporting me and giving me power. Thank you so much!